

**SUPPORT OF GULF OF MEXICO HYDRATE RESEARCH CONSORTIUM:  
ACTIVITIES TO SUPPORT ESTABLISHMENT OF A SEA FLOOR MONITORING  
STATION PROJECT**

SEMIANNUAL TECHNICAL REPORT  
1 OCTOBER, 2006 THROUGH 31 MARCH, 2007

PREPARED BY THE MANAGEMENT TEAM,  
J. Robert Woolsey, Thomas M. McGee, Carol Blanton Lutken and Elizabeth Stidham

And subcontractors:  
Bob A. Hardage, Jeffrey Chanton, Rudy Rogers, and Paul Higley and  
Laura Lapham, G. Zhang, J. Dearman, S. Xiong

**CENTER FOR MARINE RESOURCES AND ENVIRONMENTAL TECHNOLOGY**  
220 OLD CHEMISTRY BUILDING, UNIVERSITY, MS 38677  
(CONTACT: CAROL LUTKEN)

MAY, 2007

DOE Award Number DE-FC26-02NT41628

This report was prepared with the support of the United States Department of Energy, under award No. DE-FC26-02NT41628. However, any opinions, findings, conclusions, or recommendations expressed herein are those of the authors and do not necessarily reflect the views of the DOE. DOE Award Number DE-FC26-02NT41628 is managed by the U.S. Department of Energy's National Energy Technology Laboratory.

FY03 Subcontractors:

Paul Higley, Specialty Devices, Inc., 2905 Capital Street, Wylie, TX 75098

Task 1: Continuation of Work on the Vertical Line Array

J. Robert Woolsey, Mississippi Mineral Resources Institute (MMRI) and Center for Marine Resources and Environmental Technology (CMRET), 220 Old Chemistry Building, University of Mississippi, University, Mississippi, 38677

Task 2: Construction of the Prototype Sea Floor Probe

Ralph Goodman, Department of Marine Sciences, University of Southern Mississippi, 1020 Balch Blvd., Stennis Space Center, MS 39529

Task 3: Acoustic System for Monitoring Gas Hydrates

Vernon Asper, Department of Marine Sciences, University of Southern Mississippi, 1020 Balch Blvd., Stennis Space Center, MS 39529

Task 4: Construction and Testing of an Electromagnetic Bubble Detector and Counter

Boris Mizaikoff, School of Chemistry and Biochemistry, Georgia Institute of Technology, Applied Sensors Laboratory, 770 State St, Atlanta, GA 30332

Task 5: Mid-Infrared Sensor Systems for Continuous Methane Monitoring in Seawater

Angela Davis, AUGER Geophysical Services, School of Ocean Sciences, University of Wales, Bangor, Menai Bridge, Anglesey LL59 5EY, Bangor, Wales, UK

Task 6: Seismo-Acoustic Characterization of Sea Floor Properties and Processes at the Hydrate Monitoring Station

FY04 Subcontractors:

Barrodale Computing Services, Ltd. Hut R, McKenzie Avenue, University of Victoria, Victoria, BC V8W 3W2 Canada

Task 1: Data Management and Processing Software for the Sea-floor Monitoring Station

Bob A. Hardage, Bureau of Economic Geology, John A. and Katherine G. Jackson School of Geosciences, University of Texas at Austin, University Station, Box X, Austin, TX 78713

Task 2: Applications of VSP Technology for Evaluation of Deep-Water Gas Hydrate Systems\*

Jeffrey Chanton, Department of Oceanography, Florida State University, Tallahassee, FL 32306

Task 3: Coupling of Continuous Geochemical and Sea-floor Acoustic Measurements

Rudy Rogers, Swalm School of Chemical Engineering, P.O. Box 9595, Mississippi State, MS 39762

Task 4: Microbial Activity Related to Gas Hydrate Formation and Sea-floor Instabilities

FY05 Subcontractors:

Barrodale Computing Services, Ltd. Hut R, McKenzie Avenue, University of  
Victoria, Victoria, BC V8W 3W2 Canada

Task 1: Data Management and Archiving System and Matched Field  
Inversion Software Development for the Sea-floor Monitoring Station

Paul Higley, Specialty Devices, Inc., 2905 Capital Street, Wylie, TX 75098

Task 2: Experiment to generate Shear Waves in the Sea-floor and Record  
them with a Horizontal Line Array

Jeffrey Chanton, Department of Oceanography, Florida State University,  
Tallahassee, FL 32306

Task 3: Coupling of Continuous Geochemical and Sea-floor Acoustic  
Measurements

\* includes seismo-acoustic characterization of sea-floor properties and processes at the  
hydrate monitoring station until VSP data can be collected

**DISCLAIMER**

This report was prepared as an account of work sponsored by an agency of the United States Government. Neither the United States Government nor any agency thereof, nor any of their employees, makes any warranty, express or implied, or assumes any legal liability or responsibility for the accuracy, completeness, or usefulness of any information, apparatus, product, or process disclosed, or represents that its use would not infringe privately owned rights. Reference herein to any specific commercial product, process, or service by trade name, trademark, manufacturer, or otherwise does not necessarily constitute or imply its endorsement, recommendation, or favoring by the United States Government or any agency thereof. The views and opinions of authors expressed herein do not necessarily state or reflect those of the United States Government or any agency thereof.

## ABSTRACT

The Gulf of Mexico Hydrates Research Consortium (GOM-HRC) was established in 1999 to assemble leaders in gas hydrates research. The Consortium is administered by the Center for Marine Resources and Environmental Technology, CMRET, at the University of Mississippi. The primary objective of the group is to design and emplace a remote monitoring station or sea floor observatory (MS/SFO) on the sea floor in the northern Gulf of Mexico by the year 2007, in an area where gas hydrates are known to be present at, or just below, the sea floor. This mission, although unavoidably delayed by hurricanes and other disturbances, necessitates assembling a station that will monitor physical and chemical parameters of the marine environment, including sea water and sea-floor sediments, on a more-or-less continuous basis over an extended period of time. In 2005, biological monitoring, as a means of assessing environmental health, was added to the mission of the MS/SFO.

Establishment of the Consortium has succeeded in fulfilling the critical need to coordinate activities, avoid redundancies and communicate effectively among researchers in the arena of gas hydrates research. Complementary expertise, both scientific and technical, has been assembled to promote innovative research methods and construct necessary instrumentation. The observatory has now achieved a microbial dimension in addition to the geophysical, geological, and geochemical components it had already included.

Initial components of the observatory, a probe that collects pore-fluid samples and another that records sea floor temperatures, were deployed in Mississippi Canyon 118 (MC118) in May of 2005. Follow-up deployments, planned for fall 2005, had to be postponed due to the catastrophic effects of Hurricane Katrina (and later, Rita) on the Gulf Coast. Station/observatory completion, anticipated for 2007, will likely be delayed by at least one year.

These delays caused scheduling and deployments difficulties but many sensors and instruments were completed during this period. Software has been written that will accommodate the data that the station retrieves, when it begins to be delivered. In addition, new seismic data processing software has been written to treat the peculiar data to be received by the vertical line array (VLA) and additional software has been developed that will address the horizontal line array (HLA) data. These packages have been tested on data from the test deployments of the VLA and on data from other, similar, areas of the Gulf (in the case of the HLA software).

The CMRET has conducted one very significant research cruise during this reporting period: a March cruise to perform sea trials of the Station Service Device (SSD), the custom Remotely Operated Vehicle (ROV) built to perform several of the unique functions required for the observatory to become fully operational. March's efforts included test deployments of the SSD and Florida Southern University's mass spectrometer designed to measure hydrocarbon gases in the water column and The University of Georgia's microbial collector. The University of Georgia's rotational sea-

floor camera was retrieved as was Specialty Devices' storm monitor array. The former was deployed in September and the latter in June, 2006. Both were retrieved by acoustic release from a dispensable weight. Cruise participants also went prepared to recover any and all instruments left on the sea-floor during the September Johnson SeaLink submersible cruise. One of the pore-fluid samplers, a small "peeper" was retrieved successfully and in fine condition. Other instrumentation was left on the sea-floor until modifications of the SSD are complete and a return cruise is accomplished.

The seafloor monitoring station/observatory is funded approximately equally by three federal Agencies: Minerals Management Services (MMS) of the Department of the Interior (DOI), National Energy Technology Laboratory (NETL) of the Department of Energy (DOE), and the National Institute for Undersea Science and Technology (NIUST), an agency of the National Oceanographic and Atmospheric Administration (NOAA).

Subcontractors with FY03 and FY04 funding have fulfilled their technical reporting requirements in previously submitted reports. Unresolved matching funds issues remain and are being addressed in the report of the University of Mississippi's Office of Research and Sponsored Programs. In addition, Barrodale Computing Services Ltd. (BCS) completed their work for FY05; their final report is the bulk of the semiannual report, 41628R14.

Noteworthy accomplishments of Consortium researchers during this six month cycle funded with DOE's contributions to this multiagency effort include:

- Data Management and Processing Software for the Sea-floor Monitoring Station (Barrodale Computing Services Ltd. (BCS)): Completed. See 41628R14.
- Progress on the Applications of Vertical Seismic Profiling (VSP) Technology for Evaluation of Deep-Water Gas Hydrate Systems at the University of Texas Bureau of Economic Geology's Exploration Geophysics Laboratory, EGL:
  - EGL researchers have written software and processed 4-component, ocean-bottom-cable (4C OBC) seismic data to demonstrate that 4C OBC data acquired in deep water can be processed similarly to vertical seismic profile (VSP) data to yield higher-resolution images of near-seafloor geology than can be achieved with other data-processing strategies currently in use in the seismic industry.
  - The Bureau has submitted a final report of activities for this contract, included in this report.
- Progress on the Coupling of Continuous Geochemical and Sea-floor Acoustic Measurements:
  - In September 2006, the sampler box was retrieved from the sea-floor at MC118. In the following months the recovered samples, pore-fluids, were analyzed for chloride, sulfate and methane concentrations and stable

- carbon isotopic ratios.
  - Analysis showed that the northern flank of MC 118 is characterized by brine and methane-rich fluids.
  - The sampler box was replaced with a new box, ready to collect another time-series of pore-fluid samples.
  - On this same cruise, two other instrument types were deployed in the shallow sediments (<50 cm deep). Pore-water equilibration instruments (peepers) and an OsmoLander were emplaced directly adjacent to outcropping hydrate to be retrieved at a later date.
- Progress on the Microbial Activity Related to Gas Hydrate Formation and Sea-floor Instabilities:
  - This report includes the final report for this subcontract whose goal was to attempt to establish mechanisms of sea-floor hydrate formation and thereby provide guidelines that will help locate hydrates suitable for gas production.
  - Hydrate formation rates and crystal initiation times were determined for samples from various locations in MC118 and MC798. Results suggest that in near-surface sediments, sulfate zone depth, bioactivity, pore-water salinity, mineral content, bioproducts coating sediment particles, and sediment particle sizes impact hydrate nucleation and formation.
  - Sediments below the sulfate zone form hydrates more easily; the apparently random effects of gas hydrate formation in near-surface sediments may derive from different bioproducts coating the mineral surfaces in the sulfate zone. The depth of the sulfate zone is highly dependent on methane flux through the sediments
  - Smectite clays promote hydrate formation; platelets slough off the clay mass and act as nuclei for hydrate formation.
- Progress on the Experiment to Generate Shear Waves in the Sea-Floor and Record them with a Horizontal Line Array
  - Recent advances in the miniaturization of interface circuitry and support from I/O has resolved remaining engineering challenges relating to interfacing the I/O sensor to a non-I/O data collection system.
  - The possibility of using a new I/O marine DigiSeis capability was investigated, but rejected in favor of integration of the 3 component DigiSies sensor into the SDI DATS array, as previously planned, to provide for a 10-fold improvement in sampling rate.
  - I/O developed a circuit card with a proprietary custom circuitry which combines the functions of a large amount of the custom circuitry. Utilizing this new approach, SDI is building additional circuitry and writing software to resolve final communications obstacles.
- Administration of the Monitoring Station/Sea-floor Observatory project this reporting period has consisted of

- Organizing and carrying out the March cruise to test the SSD and other observatory projects.
- Organizing and facilitating the Annual Meeting of the Consortium, likely the most productive to date. All program managers were in attendance, including Traci Rodosta, the new DOE Manager and Rick Baker, our outgoing Manager for DOE. The CD of the Proceedings is available at <http://www.olemiss.edu/depts/mmri/downloads/GOM-HRC.zip><http://www.olemiss.edu/depts/mmri/downloads/GOM-HRC.zip>
- Reporting to and interacting with sponsoring agencies and their officers as well as with Consortium members. The semiannual progress report for DOE Award Number DE-FC26-02NT41628 was submitted in December and the one for DOE Award Number DE-FC26-06NT42877 was submitted in March. They are 41628R16 and 42877R02, respectively. Monthly reports have been made to DOE each month of the reporting period.



## TABLE OF CONTENTS

## PAGE

SUBCONTRACTORS.....	ii
DISCLAIMER.....	iv
ABSTRACT.....	v
TABLE OF CONTENTS.....	ix
LIST OF GRAPHICAL MATERIALS.....	ix
INTRODUCTION.....	1
EXECUTIVE SUMMARY.....	1
EXPERIMENTAL.....	6
RESULTS AND DISCUSSION.....	6
CONCLUSIONS.....	6
REFERENCES.....	7

## SUMMARIES/TECHNICAL REPORTS SUBMITTED BY THE SUBCONTRACTORS

FOR FY04 and FY05:

Task 2 (04): Applications of VSP Technology for Evaluation of Deep-Water Gas Hydrate Systems .....	8
Task 3 (04-05): Coupling of Continuous Geochemical and Sea-floor Acoustic Measurements .....	24
Task 4 (04): Microbial Activity Related to Gas Hydrate Formation and Sea-floor Instabilities .....	33
Task 2 (05): Experiment to generate Shear Waves in the Sea-floor and Record them with a Horizontal Line Array.....	55

LIST OF ACRONYMS AND ABBREVIATIONS.....	58
---	----

## LIST OF GRAPHICAL MATERIALS

Graphical materials used to illustrate reports can be found in the individual reports submitted by the subcontractors.

## **INTRODUCTION / PROJECT SUMMARY**

The Gulf of Mexico-Hydrate Research Consortium (GOM-HRC) is in its seventh year of developing a sea-floor station to monitor a mound where hydrates outcrop on the sea floor. The plan for the Monitoring Station/Sea Floor Observatory (MS/SFO) is that it be a multi-sensor station that provides more-or-less continuous monitoring of the near-seabed hydrocarbon system, within the hydrate stability zone (HSZ) of the northern Gulf of Mexico (GOM). The goal of the GOM-HRC is to oversee the development and emplacement of such a facility to provide a better understanding of this complex hydrocarbon system, particularly hydrate formation and dissociation, fluid venting to the water column, and associated microbial and/or chemosynthetic communities. Models developed from these studies should provide a better understanding of gas hydrates and associated free gas as: 1) a geo-hazard to conventional deep oil and gas activities; 2) a future energy resource of considerable significance; and 3) a source of hydrocarbon gases, venting to the water column and eventually the atmosphere, with global climate implications.

Initial funding for the MS/SFO was received from the Department of Interior (DOI) Minerals Management Service (MMS) in FY1998. Funding from the Department of Energy (DOE) National Energy Technology Laboratory (NETL) began in FY2000 and from the Department of Commerce (DOC) National Oceanographic and Atmospheric Administration's National Undersea Research Program (NOAA-NURP) in 2002. Some ten industries and fifteen universities, the United States Geological Survey (USGS), the US Navy, Naval Meteorology and Oceanography Command, Naval Research Laboratory and NOAA's National Data Buoy Center are involved at various levels of participation. Funded investigations include a range of physical, chemical, and, more recently, microbiological studies.

## **EXECUTIVE SUMMARY**

A consortium has been assembled for the purpose of consolidating both the laboratory and field efforts of leaders in gas hydrates research. The Consortium, established at and administered by the University of Mississippi's Center for Marine Resources and Environmental Technology (CMRET), has, as its primary objective, the design and emplacement of a remote monitoring station on the sea floor in the northern Gulf of Mexico by the year 2007. The primary purpose of the station is to monitor activity in an area where gas hydrates are known to be present at, or just below, the sea-floor. In order to meet this goal, the Consortium has begun assembling a station that will monitor physical and chemical parameters of the sea water, sea-floor sediments, and shallow subsea-floor sediments on a more-or-less continuous basis over an extended period of time. Central to the establishment of the Consortium is the need to coordinate activities, avoid redundancies and promote effective and efficient communication among researchers in this growing area of research. Complementary expertise, both scientific and technical, has been assembled; collaborative research and

coordinated research methods have grown out of the Consortium and design and most construction of instrumentation for the sea-floor station is essentially complete.

The MS/SFO was designed to accommodate the possibility of expanding its capabilities to include biological monitoring. A portion of FY04 funding from the MMS was directed toward this effort to support the study of chemosynthetic communities and their interactions with geologic processes. In addition, results will provide an assessment of environmental health in the area of the station. NOAA -NURP has, as a focal point, investigations of the effects of deep sea activities on world atmosphere and therefore, weather. In July of 2005, the Director of the National Institute for Undersea Science and Technology (NIUST) of NOAA-NURP made a portion of that agency's budget available *via* competitive grants to researchers with proven expertise in microbial research. A sea-floor microbial observatory is an objective of that agency and these sponsored projects sited at the MS/SFO are designed to fulfill that directive.

The centerpiece of the monitoring station, as originally conceived, is a series of vertical line arrays of sensors (VLAs), to be moored to the sea floor. Each VLA was to have extended approximately 200 meters from the sea-floor. Sensors in the VLAs include hydrophones to record water-borne acoustic energy (and measure sound speed in the lower water column), thermistors to measure water temperature, tilt meters to sense deviations from the vertical induced by water currents, and compasses to indicate the directions in which the deviations occur. During discussions among the members of the geophysical subgroup of the Consortium, it was discovered that the project may be better served if some vertical arrays are converted to horizontal line arrays (HLAs). The prospective horizontal water-bottom arrays, will consist of hydrophones and 3-component accelerometers and will be laid upon, and pressed into, the soft sediment of the sea-floor. They will be arranged into a cross so that they simulate two perpendicular arrays. Their deployment will be accomplished by means of a sea-floor sled designed to lay cable and deploy probes into shallow, unconsolidated sediments. This sled will also be used as a seismic source of compressional and shear waves for calibrating the subsurface seismo-acoustic array commissioned by the Joint Industries Program (JIP).

The prototype DOE-funded VLA has been completed and tested together with the associated data-logging and processing systems. Processing techniques continue to be developed for vertical array data by Consortium participants who are currently funded by the MMS.

In May, 2005, the Sea-Floor Probe (SFP) was used to retrieve core samples from MC118 as part of the effort to select sites appropriate for deployment of the geophysical and geochemical probes. The northwestern portion of the mound area defined on images recovered during a C&C autonomous underwater vehicle (AUV) survey April 30-May 2, 2005, was

selected for probe deployments based on information from these cores. Both the pore-fluid array and the geophysical line array were deployed *via* SFP at MC118 in May, 2005.

Additional MS/SFO deployments, scheduled for September and October, 2005, were delayed due to the devastation of the Mississippi Gulf Coast and environs by Hurricane Katrina and, to a lesser extent, the Louisiana Gulf Coast by Hurricane Rita. The immediate cause for delay was the removal of the *M/V Ocean Quest*, the vessel that, with its two submersibles, was to have provided the platform from which many of the bottom-founded sensors would have been deployed and cable connections made. It would also have provided the visual survey needed to make optimal choices of deployment sites for station components. In addition, damage to ship yards and various forms of infrastructure was been extensive.

In October, 2005, March, April and June, 2006, the CMRET conducted a series of cruises to MC118 aboard the *R/V Pelican*. These cruises accomplished many of the tasks that had been planned for the *Ocean Quest*, including the recovery of more samples from MC118 and the deployment of a microbial filter device. A complete SS/DR (surface-source/deep-receiver) survey was made and a drift camera designed, deployed and used successfully to survey the sea-floor, visually. However, a submersible or ROV was still required to accomplish many of the missions for which precise placement of instruments on the sea-floor was required.

Following several “false starts”, anticipating the use of other vessels which never did become available, the CMRET eventually secured seven days of ship time aboard the *R/V Seward Johnson* with use of its manned-submersible, the Johnson SeaLink. This vessel combination was used to retrieve the osmopump packages and data-loggers deployed in 2005, to conduct visual surveys of the observatory site at MC118 and to deploy, and in some cases recover, sensors and experiments. Experiments designed to assess microbial communities and activities, hydrate host materials, and composition of pore-fluids were left on the sea-floor for several months’ data collection. Cruises to recover these instruments and data-loggers have already been scheduled for 2007.

Delays attributable to hurricane activity in the Gulf of Mexico caused scheduling and deployments difficulties but many sensors and instruments were completed during this period. A second PFA osmosampler was placed on the sea-floor near the southwestern crater at the site designated “Rudyville”. Pore water equilibrators or “peepers” were installed at three sites at MC118. In addition to samples and data collected from these instruments, methane concentration and isotope samples were collected from 8 cores that were collected using the SeaLink at a variety of sites along transects across microbial mats.

After 1.5 years, the Pore-Fluid Array's (PFA's) instrument package was recovered and replaced successfully during the September Johnson SeaLink dives. The four ports collecting pore-fluids via OsmoSamplers were located in the overlying water and 1.2 m, 3.2 m, and 8.5 meters below the seafloor (mbsf). During the months following the retrieval of the sample box, pore-fluids were extracted from the sampler coils and measured for chloride, sulfate, and methane concentrations and methane isotope ratios. Normal seawater conditions were found in the overlying waters, while at 8.5 mbsf, chloride concentrations provide compelling evidence for the intrusion of brine fluids. Brine was further indicated by the absence of sulfate. As expected with brine fluids, they were also characterized by high methane concentrations.

Defining mechanisms of sea-floor hydrate formation to aid in locating hydrates on the sea-floor is a long-term component of Consortium efforts. A final report, included in this report, includes the results of laboratory findings relating to hydrate induction time and formation rates. A significant finding of this study is that hydrate formation is catalyzed by biosurfactants, products of microbial activity. The microbes' bioproducts' hydrophobic moieties collect methane while the hydrophilic moieties collect and structure water, thus emplacing the components necessary for hydrate formation. This in turn, explains the close affiliation of particular bacteria with hydrate outcrops on the sea-floor and leads to further questions regarding their interactions. Some generalizations can be made regarding hydrate formation: formation rates increase with depth until a maximum is reached and induction time decreases with depth until a minimum is reached. These generalizations are influenced, and in some cases overcome, by other factors influencing hydrate formation such as salinity, the depth of the sulfate zone, salinity, bioactivity, clay mineral composition, bioproducts coating sediment grains, and sediment size.

Software has been written that will accommodate the data that the station retrieves, when it begins to be delivered. In addition, new seismic data processing software has been written to treat the peculiar data to be received by the vertical line array (VLA) and additional software has been developed that will address the horizontal line array (HLA) data. These packages have been tested on data from the test deployments of the VLA and on data from other, similar, areas of the Gulf (in the case of the HLA software).

Researchers at the Exploration Geophysics Laboratory (EGL) have developed a new approach to processing 4-component (4C) seismic data acquired with multicomponent sensors deployed on the seafloor. Utilizing the large elevation difference between source and receiver allows deep-water 4C data to be processed with algorithms similar to those used to make images from vertical seismic profile (VSP) data (also acquired with a large elevation difference between source and receiver). This processing approach produces images that have much higher resolution of geology located near the receiver station than do standard 4C data-processing techniques.

New 4C OBC seismic data-processing software structured to optimize image resolution in the immediate vicinity of seafloor seismic sensors has been written by EGL researchers. While this novel data-processing strategy offers no advantage for imaging deep geology, it produces optimal images of geology immediately below seafloor sensor stations where hydrate systems are embedded. Preliminary tests of this software have produced impressive high-resolution images of near-seafloor strata.

The problem of integrating the Input/Output (I/O) sensor – with superior resolution, accuracy and low frequency response to that of marine 3 axis geophone sensors - to the Horizontal Line Array appears to be resolved. Recent advances in the miniaturization of interface circuitry and support from I/O has resolved the remaining engineering tasks and trial collection of 4C data will be completed in June 2007.

The possibility of using a new I/O marine DigiSeis capability was investigated. The advantage of this system is that the marine version of this sensor has a hydrophone integrated with the three axis accelerometer. The drawback is that the present hydrophone sample rate is limited to 1 ms (1,000sps) and the effort involved in redesigning the system to achieve the desired 10,000 sps rate would require more investment than the entire borehole vertical array program's present budget. The decision was made to stay with integration of the 3 component DigiSies sensor into the SDI DATS array.

SDI is building additional circuitry and writing software to finally resolve further communications and power challenges. New circuitry has apparently cured the last of the problems for packaging this technology in a format that will lend itself to installation on the sea floor. The new combination of cards and software is being packaged and will be tested at sea with the MMRI Sled combination S and P wave source in June.

The CMRET conducted a critically important research cruise during this reporting period: a March cruise to perform sea trials of the Station Service Device (SSD), the custom Remotely Operated Vehicle (ROV) built to perform several of the unique functions required for the observatory to become fully operational. Initial requirements for the SSD included deployment and recovery of tools and sensors and the connection of underwater-mateable electric and fiber optic connectors at depth. The standard complement of equipment included: high resolution video with lighting, scanning sonar, robotic arm, precision positioning and thrusters for limited transit and maneuvering. The winch, tether and umbilical cable carry an optical fiber that provides video, scanning sonar, and vehicle attitude information to the operator and carry commands to the SSD tether winch, thruster control and robotic arm operations.

March's cruise accomplishments included test deployments of the SSD, Florida Southern University's mass spectrometer designed to measure hydrocarbon gases in the water column and The University of Georgia's microbial collector. The University of Georgia's rotational sea-floor camera was retrieved as was Specialty Devices' storm monitor array. The former was deployed in September and the latter in June, 2006. Both were retrieved by acoustic release from a dispensable weight. Cruise participants also went prepared to recover any and all instruments left on the sea-floor during the September Johnson SeaLink submersible cruise. One of the pore-fluid samplers, a small "peeper" was retrieved successfully and in fine condition. Other instrumentation was left on the sea-floor until modifications of the SSD and support vessel are complete and a return cruise is accomplished.

Reporting to and interacting with sponsoring agencies and their officers as well as with Consortium members is a primary administrative function of CMRET. The semiannual progress report for DOE Award Number DE-FC26-02NT41628 was submitted in December and the one for DOE Award Number DE-FC26-06NT42877 was submitted in March. They are 41628R16 and 42877R02, respectively. Regular monthly reports documenting progress of subcontractors as well as the Consortium in general were also submitted.

Wall-to-Wall, an independent television programming production company under contract to Discovery Television to produce the miniseries, *Building the Future* (previously *Surviving the Future*) has rescheduled their installment, *Energy*, for which they filmed portions of the September Johnson SeaLink cruise. The broadcast is currently scheduled to air in June, 2007.

## **EXPERIMENTAL**

Experiments are described in the individual reports submitted by the subcontractors.

## **RESULTS AND DISCUSSION**

Results and discussion of those results are described in the individual reports submitted by the subcontractors. Reports from the subcontractors follow.

## **CONCLUSIONS**

This report covers the accomplishments of the six-months from October 1, 2006 through March 31, 2007 for Cooperative agreement Project #DE-FC26-02NT41628, between the Department of Energy and the Center for Marine Resources and Environmental Technology, University of Mississippi. The efforts of the Hydrates Research Consortium are reviewed; at-sea activities reported; laboratory and computational projects reviewed. Two projects, *Applications of VSP Technology for Evaluation of Deep-Water Gas-Hydrate Systems* and *Microbial Activity Related to Gas Hydrate Formation and Seafloor Instabilities*

were completed and researchers' final reports submitted. These are included in this report. Retrieval of instruments from the SFO site has begun and ground-breaking data and implications have begun to be realized. Deployments of additional station components are anticipated for the remainder of 2007.

Ship time remains tight in the Gulf. Cessation of DOE and MMS funding for this project has created a crisis in the Sea-floor Observatory completion schedule. In particular, while the CMRET has 18 more days of ship time scheduled aboard the *R/V Pelican* in 2007, rebudgeting of existing funds will be necessary in order to use these cruise days. Every effort has been – and will continue to be – made to maximize Consortium members' access to and benefit from the cruises scheduled for 2007.

Project summaries of the subcontractors' efforts appear in their reports contained within this document. All FY03 subcontractors have completed their technical reporting although financial reports are not yet complete. The CMRET continues to work with the sponsored programs officials at several institutions to resolve these delays, most of which involve incorrect reporting of cost-sharing. The VLA and the SFP are complete and have been proven. Software development and innovative processing techniques are complete until additional sensor details become available. The "bubble counter" is complete and was successfully deployed on the September 2006 cruise. Laboratory studies of gas hydrates have shown a direct link between microbial bioproducts and formation of gas hydrates. Additional influences on gas hydrate formation and stability have been identified and their impacts demonstrated.

The pore-fluid sampling probe and thermistor geophysical probe, emplaced on the sea floor in May of 2005, have been recovered in good condition with samples and data-loggers intact. The data-logger and sample-collecting box of these components contain the first data produced at the MS/SFO. Analyses of pore fluid samples from this deployment are discussed in the report that follows. One remarkable find is that the salinity of the subsurface pore-fluids is ~8 times that of normal sea-water and may explain the lack of gas hydrates – whose formation is known to be inhibited by the presence of brine – at the northern vent site.

The Consortium continues to establish and foster cooperations through semiannual meetings and cruises. The March cruise resulted in several successful tests, notably that of the Station Service Device, the custom ROV designed to perform various observatory functions including making and breaking connections, emplacing and retrieving instruments from the sea-floor and performing local surveys.

## **REFERENCES**

Relevant references appear following contributions by the individual subcontractors.



***Support of Gulf of Mexico Hydrate Research Consortium:  
Activities to Support Establishment of Seafloor Monitoring  
Station***

**DOE Cooperative Agreement No. DE-FC26-02NT41628**

**Applications of VSP Technology for Evaluation  
of Deep-Water Gas-Hydrate Systems**

**FINAL REPORT**

Reporting Period Start Date: October 1, 2006

Reporting Period End Date: March 31, 2007

Principal Investigator (Author): Bob A. Hardage

Date Issued: May 14, 2007

Submitting Organization:  
Bureau of Economic Geology  
John A. and Katherine G. Jackson School of Geosciences  
The University of Texas at Austin  
University Station, Box X  
Austin, TX 78713-8924

## **Abstract**

We have written software and processed 4-component, ocean-bottom-cable (4C OBC) seismic data to demonstrate that 4C OBC data acquired in deep water can be processed as vertical seismic profile (VSP) data to yield higher-resolution images of near-seafloor geology than can be achieved with other data-processing strategies practiced across the seismic industry.

## **Table of Contents**

- Abstract
- Introduction
- Executive Summary
- Experimental
- Results and Discussion
  - 4C OBC Sensor Concepts
  - Conventional Data Processing of 4C OBC Data
  - New VSP Data Processing Approach
  - P-P and P-SV Reflectivities
  - Constructing P-P and P-SV Images
  - Image Comparisons
- Conclusions
- References
- Abbreviations and Acronyms

## **List of Figures**

- Figure 1. 4C OBC data acquired at a single station
- Figure 2. Basic responses of 4C ocean-bottom sensors
- Figure 3. Comparison of P-P images
- Figure 4. Comparison of VSP and OBC geometries
- Figure 5. VSP-deconvolved P-P data
- Figure 6. VSP-deconvolved P-SV data
- Figure 7. Autonomous Underwater Vehicle technology
- Figure 8. Chirp-sonar data acquired with AUV system
- Figure 9. Comparison of P-SV image and AUV image
- Figure 10. Depth-registered P-SV and AUV images

## **Introduction**

Researchers at the Exploration Geophysics Laboratory (EGL) have developed a new approach to processing 4-component (4C) seismic data acquired with multicomponent sensors deployed on the seafloor. This new data-processing philosophy takes advantage of the large elevation difference between the seismic source (on the sea surface) and the seismic receiver (on the seafloor) that is involved in deep-water data acquisition. This large elevation difference between source and receiver allows deep-water 4C data to be processed with algorithms similar to those used to make images from vertical seismic profile (VSP) data, which are also acquired with a geometry in which there is a large elevation difference between source and receiver. This VSP data-processing approach for 4C ocean-bottom-cable (OBC) data produces images that have much higher resolution of geology located near the receiver station than do standard 4C data-processing techniques.

## **Executive Summary**

New 4C OBC seismic data-processing software has been developed at EGL that is structured to optimize image resolution in the immediate vicinity of seafloor seismic sensors. This data-processing strategy offers no advantage for imaging deep geology far below the seafloor, but it creates optimal images of geology immediately below seafloor sensor stations where hydrate systems are embedded. Preliminary tests of this software have produced impressive high-resolution images of near-seafloor strata.

## **Experimental**

Experimental activity during the funding period focused on developing and testing software that allows 4C OBC data to be used to make improved P-P and P-SV images of near-seafloor geology.

## **Results and Discussion**

### **4C OBC Sensor Concepts**

A 4C OBC receiver station has four sensing elements: a hydrophone (**P**), a vertical geophone (**Z**), a horizontal radial geophone (**X**), and a transverse horizontal geophone (**Y**). Typical responses of these four sensing elements at an arbitrary receiver station along an OBC profile that was analyzed in this study are illustrated as Figure 1. Because these data were acquired as 2D data, the response of the transverse horizontal geophone **Y** for reflections generated near the seafloor is small compared to the response of the inline horizontal geophone **X**. Thus the **Y** geophone data are ignored in the analysis that we did in the Gulf of Mexico (GOM). In other locations, the response of the **Y** geophone may need to be considered.

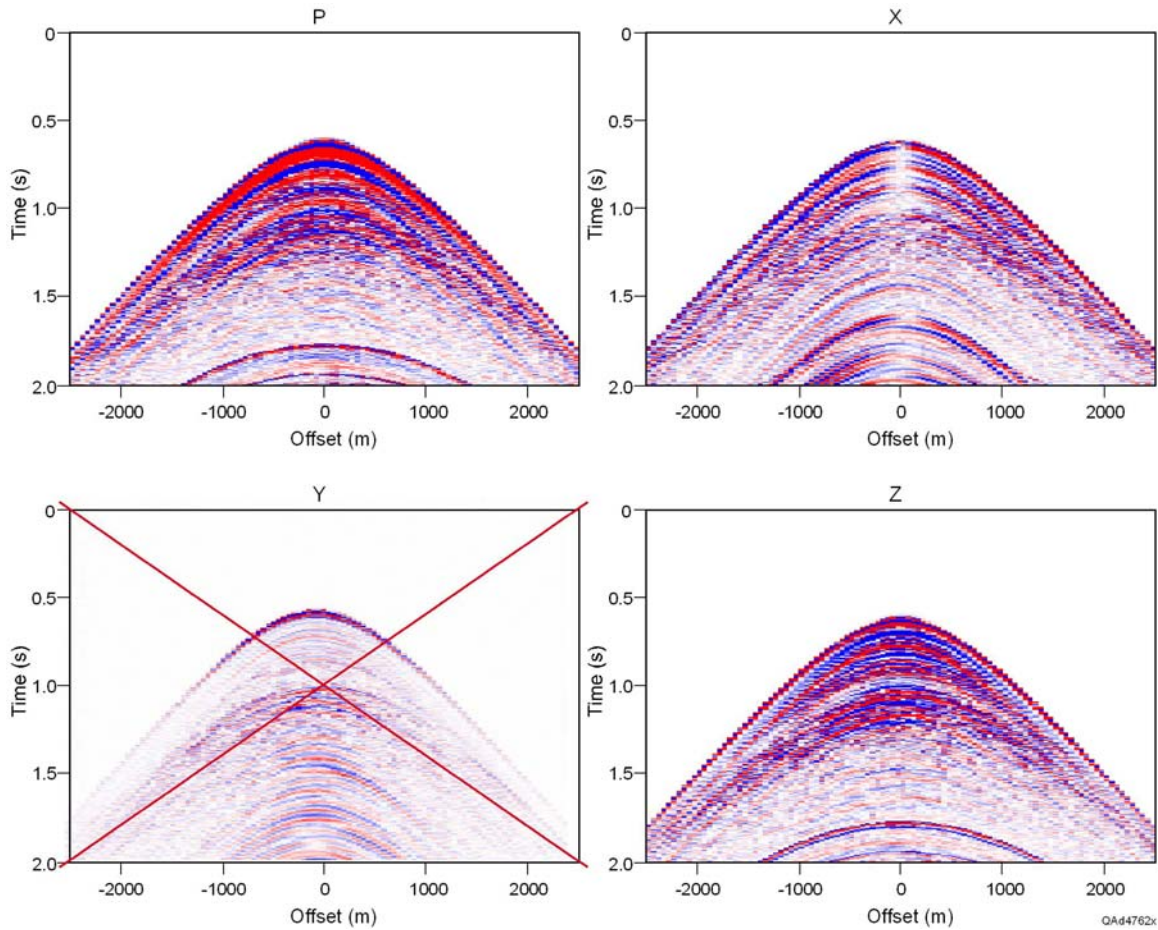


Figure 1. 4C OBC data collected at a single receiver station. Source spacing is 50 m. The sea-bottom multiple appears at normal incidence time of 1.75 seconds. The water-column multiple dominates the PP section when it arrives, but we can ignore this multiple because since it is positioned below our gas hydrate target zone. However, the multiple appears on the **X** (radial) component section and interferes with PS reflections arriving between 1.6 and 2 seconds. These PS events image strata in the range of gas hydrate interest, 130-200 m below the seafloor. In most 2D 4C OBC data, the transverse **Y** component is usually low amplitude and can be ignored in the normal data-processing flow. These data extend only to 2 seconds. **P** is the hydrophone response; **Z** is the response of the vertical geophone.

A numerical model of the response of each sensing element of a 4C receiver that explains this observed data behavior is shown as Figure 2. The three sensor-response equations for **P**, **Z**, and **X** defined in this diagram are key to the theory of our VSP-based software development. Because the shallow **Y** data can be ignored in the 4C OBC profiles that we have examined, no response equation is listed for the **Y** sensor. In these equations, **D** is the downgoing wavefield, and **U** is the upgoing wavefield.

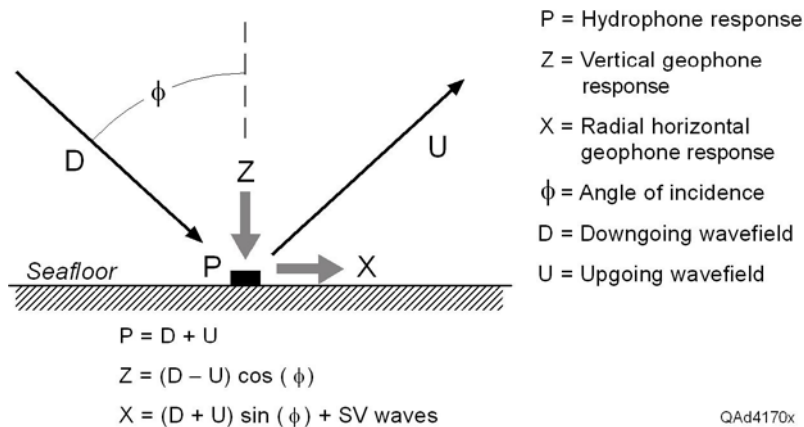


Figure 2. Basic responses of 4C ocean-bottom sensors. The three response equations are keys to the imaging theory illustrated in this report. We assume the response of the **Y** (transverse) horizontal geophone can be ignored. This assumption is correct for the data used in this report but needs to be verified at each study site. A second assumption is that the  $V_P/V_S$  velocity ratio is high, which positions the P-to-SV conversion point almost directly beneath the seafloor receiver station. As a result, the upgoing SV ray path is almost vertical, and essentially all of the SV response is on inline horizontal geophone **X**. The SV wavefield can then be separated from the **X** response by appropriately calibrating and weighting the **P** response and subtracting it from **X**. We determine the wavefield to subtract from **X** by calculating a constrained cross-equalization filter to change **P** to **X**.

## Conventional Data Processing of 4C OBC Data

In deep-water multicomponent seismic data acquisition, there is a large elevation difference between source stations (an air gun towed near the sea surface) and receiver stations on the seafloor. Conventional processing of deep-water 4-C seismic data involves a wave-equation datuming step which transforms the data to a domain in which sources and receivers are on the same depth plane. This step effectively removes the water layer and allows the data to be processed as if the source was on the seafloor. This adjustment of source-receiver geometry allows deep-water multicomponent data to be processed with software already developed for shallow-water environments where marine multicomponent data acquisition technology was originally developed and applied. An example of a good-quality, deep-water P-P image of near-seafloor geology made with this wave-equation datuming approach is shown as Figure 3a. This image shows local geology associated with a fluid-gas expulsion chimney that extends to the seafloor.

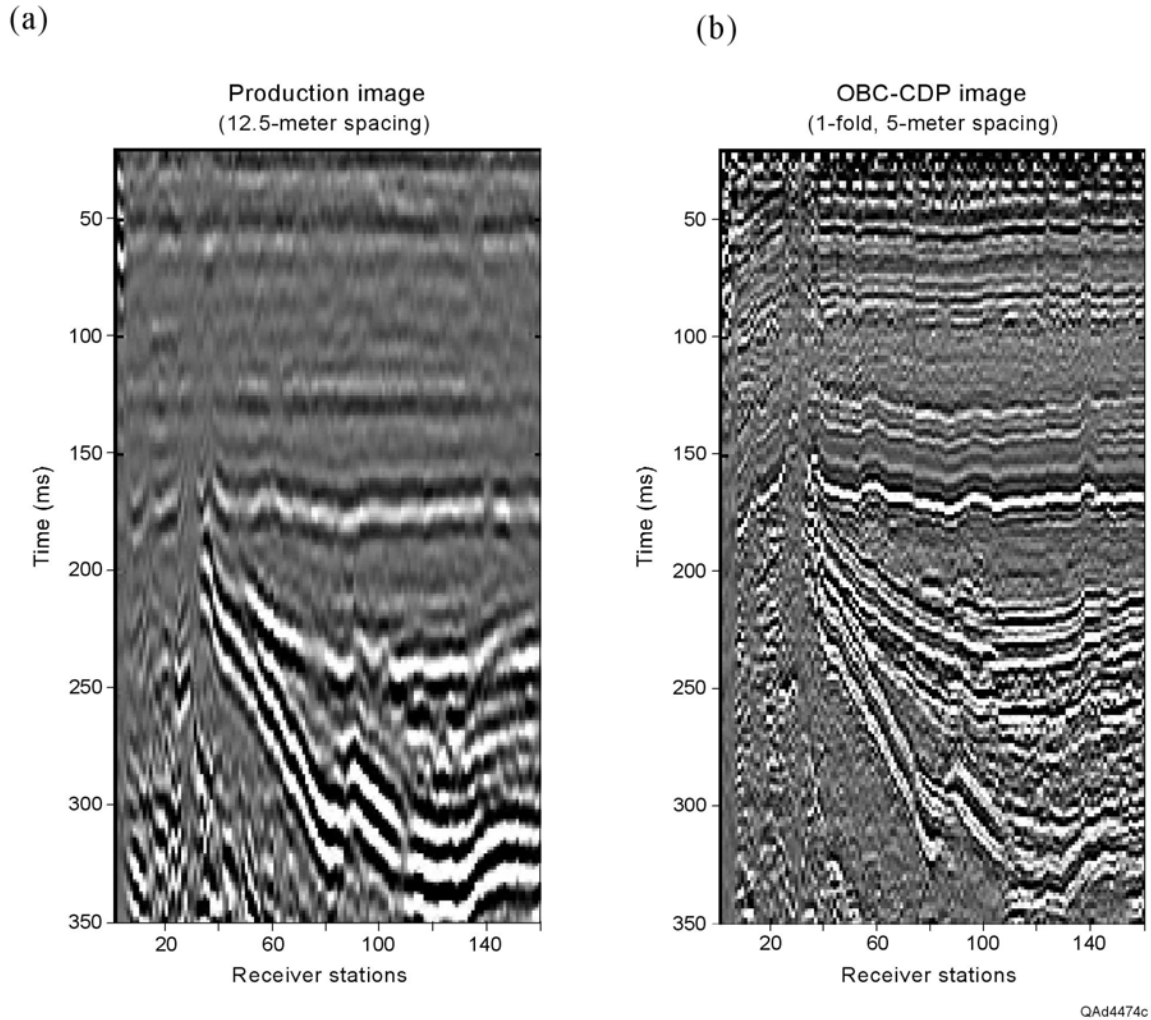


Figure 3. (a) Standard production processing of deep-water 4-C OBC seismic data along a profile that traverses a seafloor gas-expulsion chimney. (b) Improved resolution of near-seafloor geology using VSP-style concepts for processing deep-water OBC data. Both images are flattened to the seafloor.

### New VSP Data-Processing Approach

If a person wishes to study near-seafloor strata in greater detail, a new approach to P-P and P-SV imaging of deep-water multicomponent seismic data is to not eliminate the large elevation difference between sources and receivers as is done in wave-equation datuming but to take advantage of that elevation difference. The objective is to process deep-water multicomponent data similar to the way vertical seismic profile (VSP) data are processed, because VSP data acquisition also involves large elevation differences between sources and receivers (Fig. 4). Users of VSP technology know VSP data provide high-resolution images of geology near downhole receiver stations. That same logic leads to the conclusion that deep-water multicomponent seismic data processed with VSP-style techniques should yield higher resolution images of geology near

deep seafloor receivers, which is the domain of deep-water hydrate systems. Results of this software research have been described by Backus and others (2006) and by Hardage and Murray (2006a, 2006b).

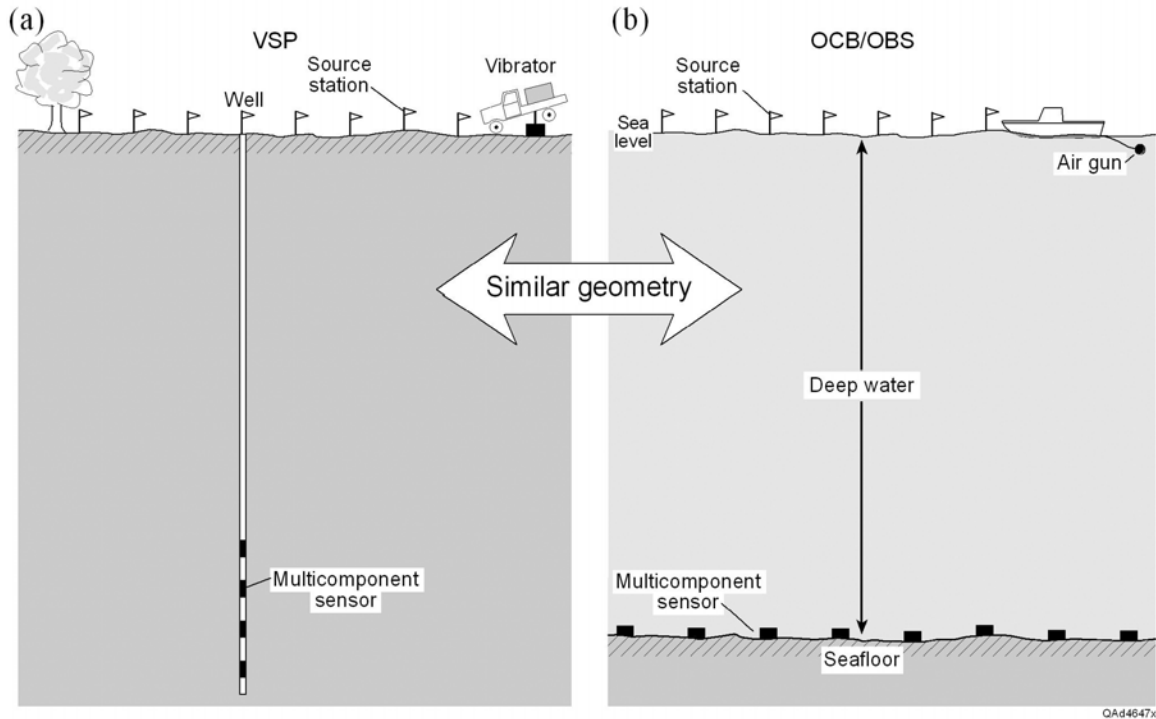


Figure 4. Illustration of similar source-receiver geometries used for acquiring (a) VSP data and (b) deep-water OCB/OBS seismic data.

## Creating Downgoing and Upgoing Wavefields

The P-SV data processing that will be illustrated can be done only with 4C data because it is essential to have data acquired with a horizontal radial **X** geophone. However, the P-P processing illustrated here can be done with either 2-C or 4-C seafloor sensors. The fundamental requirement for P-P imaging is to acquire data with a sensor having a hydrophone and a vertical geophone. Referring to the basic equations listed in Figure 2, the seafloor hydrophone response (**P**) and the seafloor vertical-geophone response (**Z**) are combined to create downgoing (**D<sub>P</sub>**) and upgoing (**U<sub>P</sub>**) P-P wavefields as:

$$(1) D_P = P + Z/\cos(\Phi)$$

$$(2) U_P = P - Z/\cos(\Phi)$$

$\Phi$  defines the incident angle at which the downgoing compressional wave arrives



at the seafloor.

Referring to the response equation for the **X** sensor in Figure 2, the upgoing P-SV wavefield **U<sub>SV</sub>** can be expressed as,

$$(3) \quad \mathbf{U}_{SV} = \mathbf{X} - (\mathbf{P}_{est}) \sin(\Phi),$$

where **P<sub>est</sub>** is the response of the **P** sensor (top equation of Figure 2) after the amplitude and phase of the **P** data are adjusted to match the amplitude and phase of the **X** data. Once these wavefield separations are done, deep-water P-P and P-SV seismic data are defined in terms of downgoing and upgoing wavefields just as VSP data are.

### **P-P and P-SV Reflectivities**

Having access to downgoing **D<sub>P</sub>** and upgoing **U<sub>P</sub>** and **U<sub>SV</sub>** wavefields means sub-seafloor P-P and P-SV reflectivities can be determined, respectively, by the ratios,

$$(4) \quad R_P = U_P/D_P$$

$$(5) \quad R_{SV} = U_{SV}/D_P.$$

These ratios are calculated in the frequency domain and then inverse Fourier transformed to the image-time domain. In the image-time domain, **R<sub>P</sub>** describes the P-P reflectivity behavior of sub-seafloor strata, and **R<sub>SV</sub>** defines the P-SV reflectivity behavior of these same strata. The ratios in Equations 4 and 5 are commonly referred to as “*VSP deconvolution*” hence the link between standard VSP data processing and our new approach to processing deep-water 4C OBC data.

### **Constructing P-P and P-SV Images**

The ratios defined in Equations 4 and 5 are calculated for each common-receiver gather at each receiver station along an OBC profile. A typical common-receiver gather is illustrated in Figure 1. Once this calculation is done, we have defined P-P and P-SV reflectivities at each receiver station. The next task is to convert these reflectivities into images. This imaging procedure is identical to the **VSP walkaway** technique that has been practiced for more than two decades in the VSP data-processing industry. Basically, each reflectivity result at each receiver station is segregated into depth-offset stacking corridors. An example of P-P depth-offset stacking corridors determined at one receiver station is illustrated as Figure 5, and an example of P-SV depth-offset stacking corridors calculated at the same receiver station is shown in Figure 6.

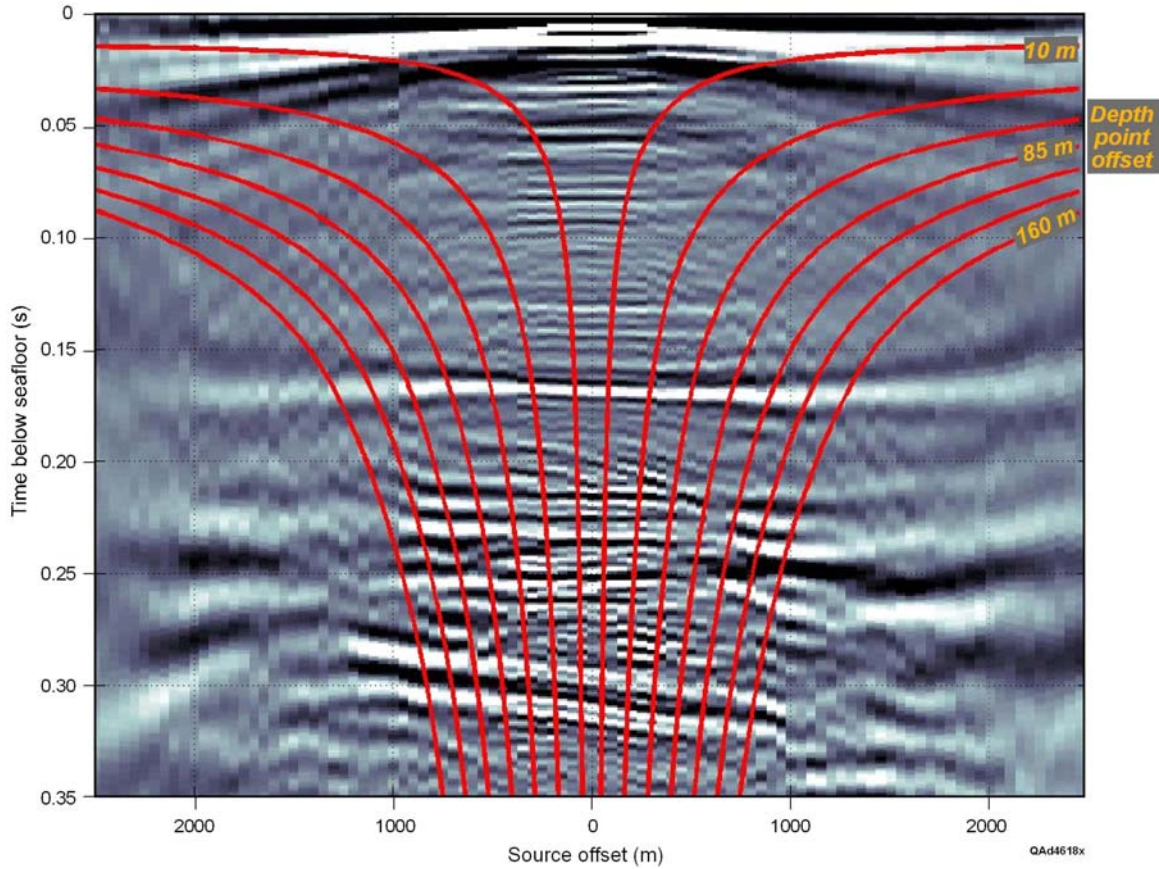


Figure 5. VSP-deconvolved P-P data at a single receiver station after application of ray-trace-based, dynamic time corrections calculated for a flat-layered Earth model of near-seafloor strata. The red lines define the location of data at fixed depth-point offsets from the receiver location. Offsets are shown at  $\pm 10$  to  $\pm 160$  m at 25-m intervals. For Figure 3b, we interpolated five traces at 5-m intervals from -10 to +10 m of depth-point offset. These five traces are interpolated between the two interior red lines in the figure. Data between the two outer red lines show subsurface structure from 160 m left of a receiver station to 160 m right of the station. Since these are common-receiver data rather than common-depth-point data, the events are not flat.

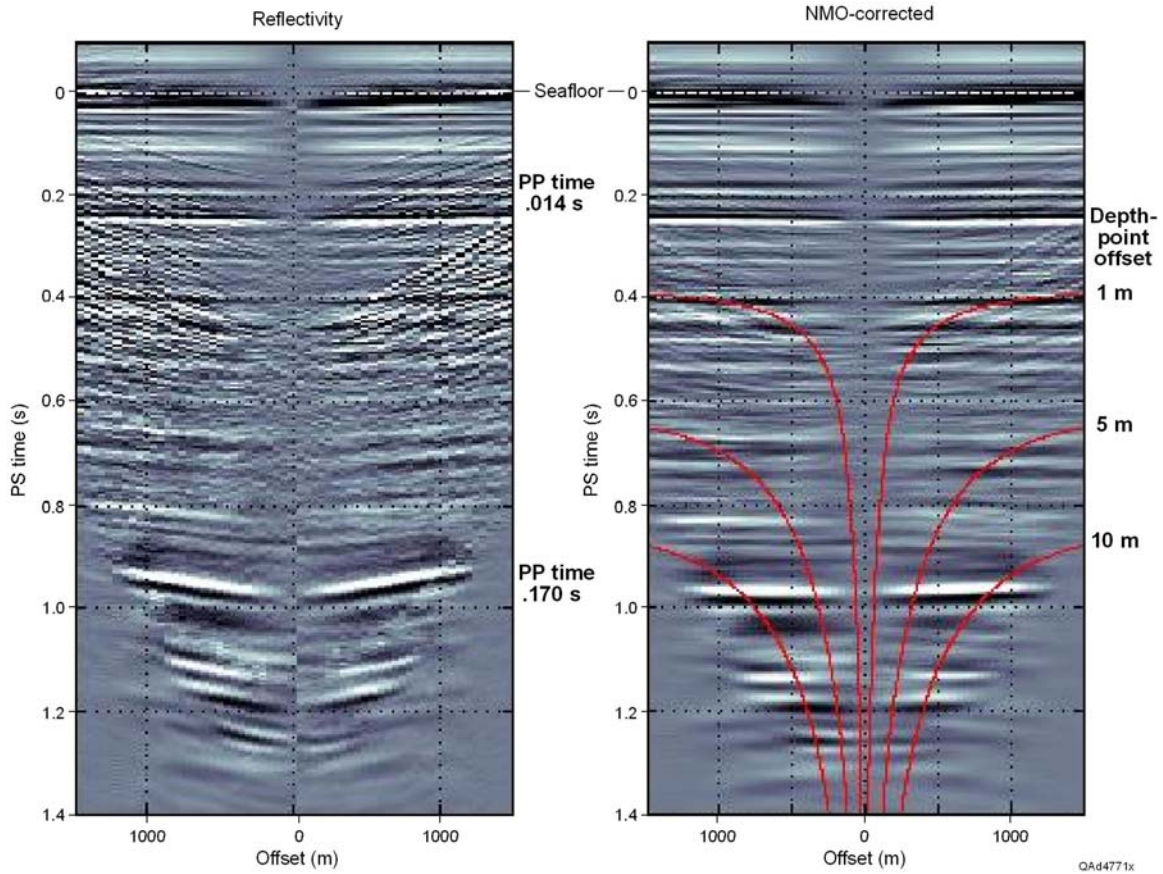


Figure 6. VSP-deconvolved P-SV data at the same receiver station used in Figure 5 before and after dynamic moveout correction. A 5-trace mix was applied on the right panel. 1-, 5-, and 10-m depth point offset lines are shown in red on the right. For depth-registration purposes, P-P reflector times of .014 and .170 seconds are shown at P-SV times of .25 and .98 seconds. In the depth range covered by our high-frequency AUV P-P data, subsurface coverage at a single receiver is less than  $\pm 2$  m. For this reason, the trace spacing in our P-SV images is 25 m, the same interval as the receiver station spacing. Note that in contrast to the P-P reflectivity, the P-SV moveout is small, and there is no moveout stretch problem.

## Image Comparisons

Figure 3b shows a P-P image made with our new VSP-based data-processing technique using the same deep-water data displayed in Figure 3a. The improvement in resolution that results with our procedure is obvious.

To show the spectacular resolution of the P-SV images constructed with this new data-processing approach, we have to utilize high-frequency P-P data acquired with Autonomous Underwater Vehicle (AUV) technology. An illustration of an AUV survey is shown in Figure 7. The AUV module is self-propelled, guided by GPS technology, travels approximately 50 m above the seafloor, and illuminates the seafloor with the wavefields listed in the diagram (side-scan sonar, multibeam bathymetry, and chirp-sonar). The chirp-sonar data are of

particular interest because these data are a P-P signal that spans a frequency sweep from 2 to 10 kHz. These high-frequency data penetrate only 40 or 50 m into the seafloor sediment, but they provide a high-frequency P-P image of near-seafloor strata across this penetration interval.

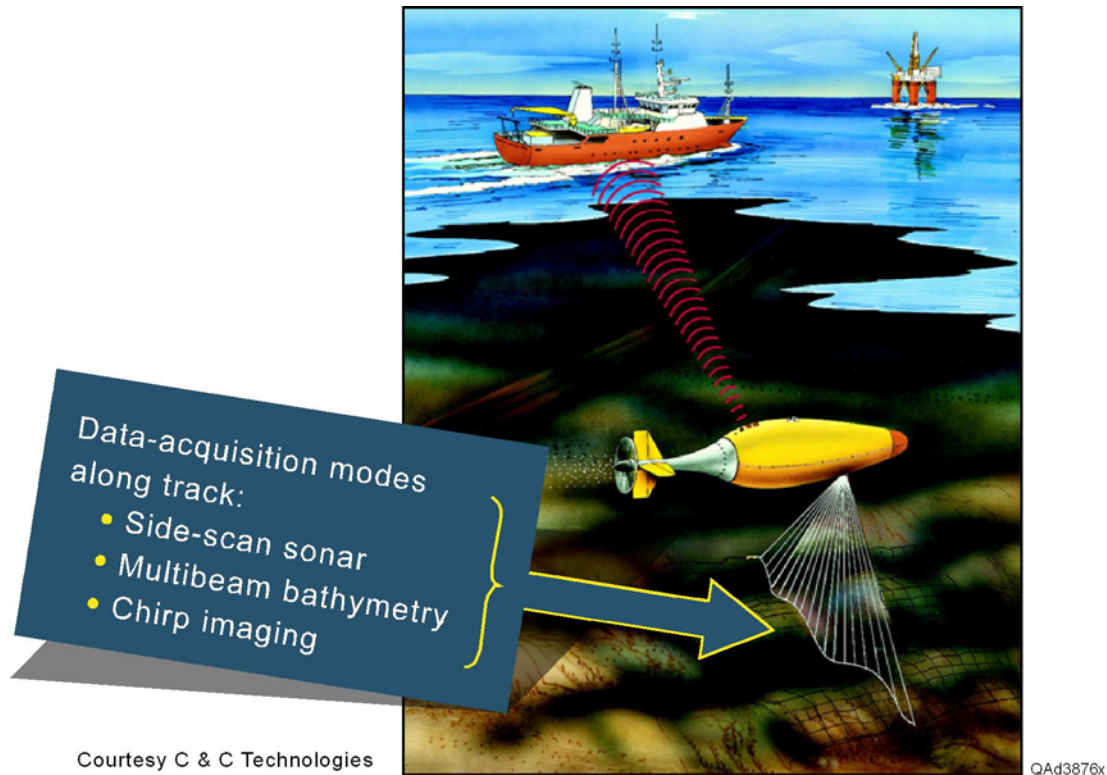


Figure 7. Seafloor imaging with an Autonomous Underwater Vehicle (AUV).

AUV chirp-sonar data acquired along one OBC test profile are displayed as Figure 8. The bottom panel shows the data as recorded and illustrates the seafloor topography. The top panel shows the data after they are shifted to a flat seafloor datum. The unconformity that occurs at about 8 ms below the seafloor is more obvious in the top panel. The P-wave velocity  $V_P$  across this near-seafloor interval is approximately 1500 m/s, not significantly different from the P-wave velocity in sea water. Using this value for  $V_P$ , the shallow interface at 2ms (top panel) is approximately 1.5 m below the seafloor, and many of the vertical throws of the faulted strata is less than 1 m.

In Figures 9 and 10, we compare zoom windows from this high-frequency AUV P-P profile with similar zoom windows of the low-frequency (10 to 150 Hz) air-gun source P-SV image we constructed with our VSP-style data-processing strategy. Inspection of these images shows that the air-gun-source P-SV data



have a spatial resolution equivalent to kilohertz-range P-P data. We consider this result to be a spectacular confirmation of the value of this new VSP-type data-processing approach for 4C OBC data that are to be used to analyze deep-water hydrate systems.

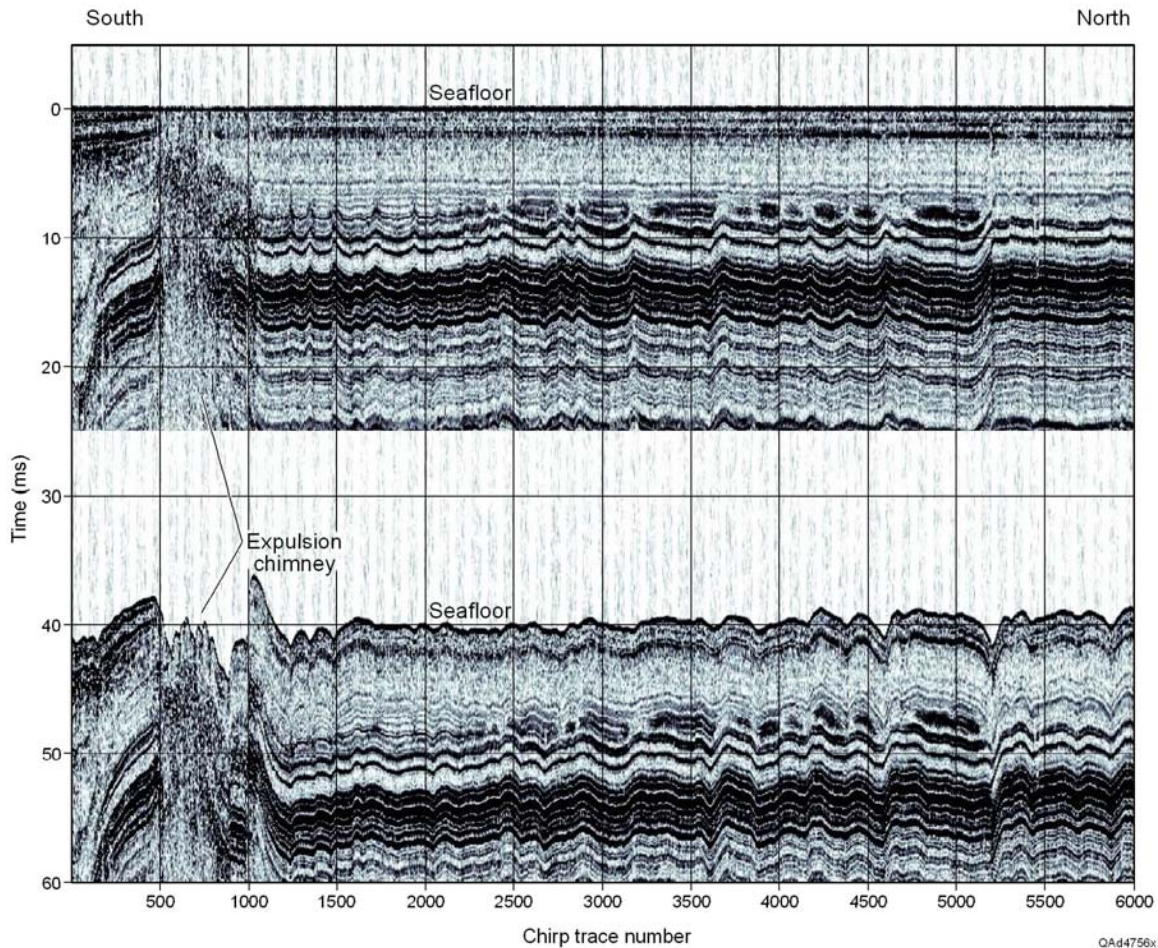
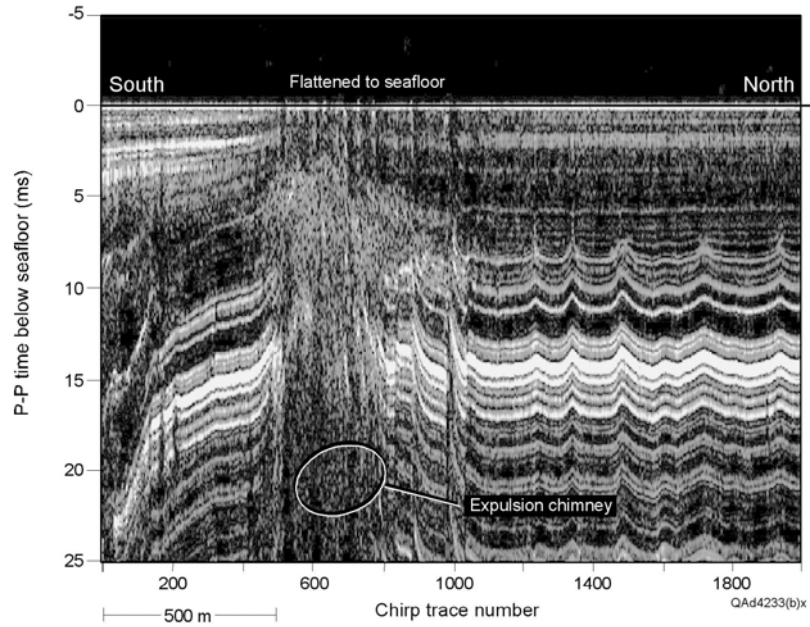


Figure 8. The PP image provided by a high-resolution AUV system along the same OBC profile illustrated in Figure 3. The 6000 traces in this image extend 6 km (1 m trace spacing). The upper panel shows the AUV data corrected to a seafloor datum. The lower portion shows the data as recorded, with the AUV following a traverse about 50 m above the ocean floor. Note the strong event about 2 ms (1.5 m) below the seafloor. This event corresponds to the P-SV reflection 60 ms below the seafloor in Figure 10b. Below 7 ms there is an obvious, abrupt unconformity that serves as an excellent marker for registration with the P-SV section at 150 ms (Fig. 10b). This unconformity is less obvious in the lower image.

(a)



(b)

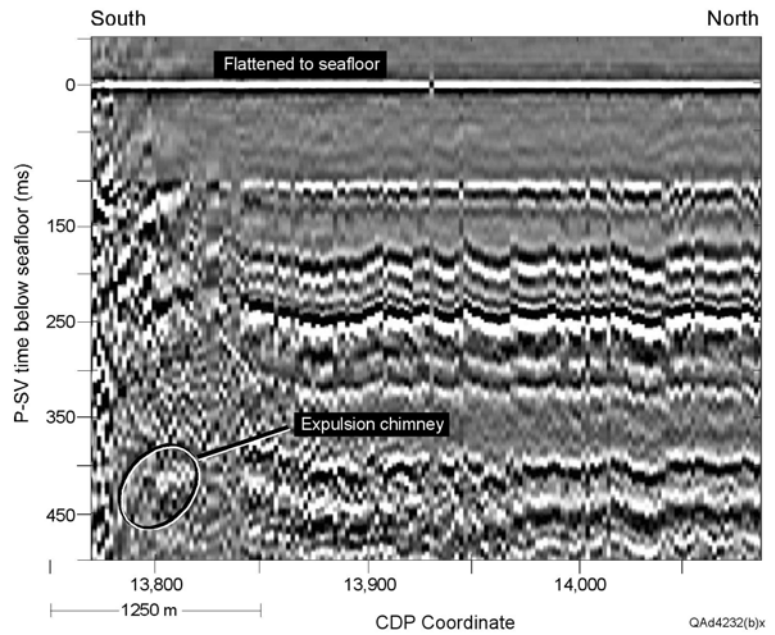
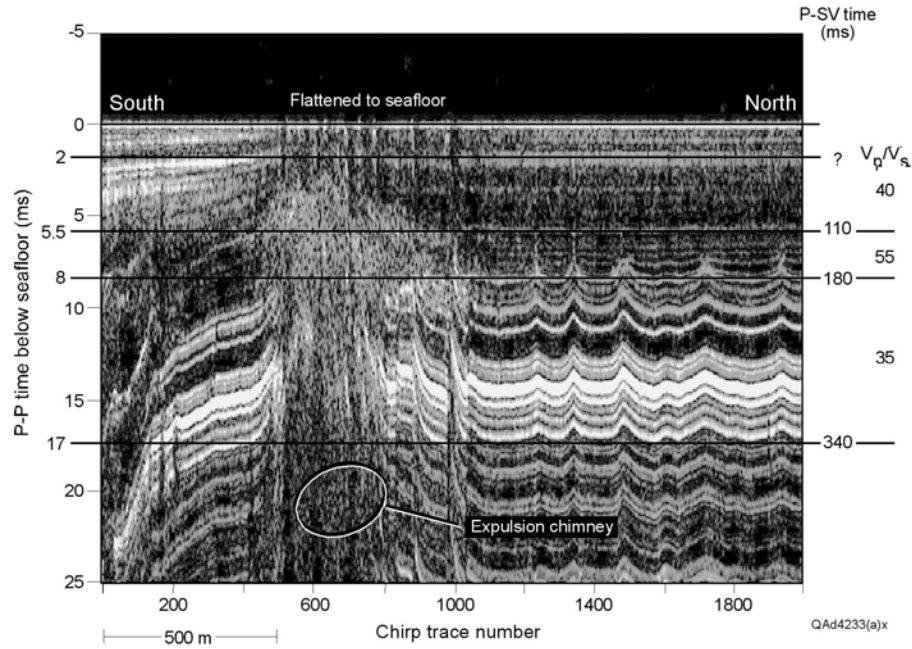


Figure 9. (a) High-frequency (2-10 kHz) AUV P-P image of near-seafloor strata across a fluid expulsion chimney. (b) Low-frequency (10-150 Hz) P-SV image produced by our new VSP-based code along the same profile. Visual comparisons show the images have equivalent spatial resolutions and thus equivalent wavelength spectra. The south end of the P-SV profile starts at about AUV chirp-trace number 700. These images have been flattened to the seafloor which causes small-throw faults (throws of 1 meter and less) to appear as chevron-shaped patterns.

(a)



(b)

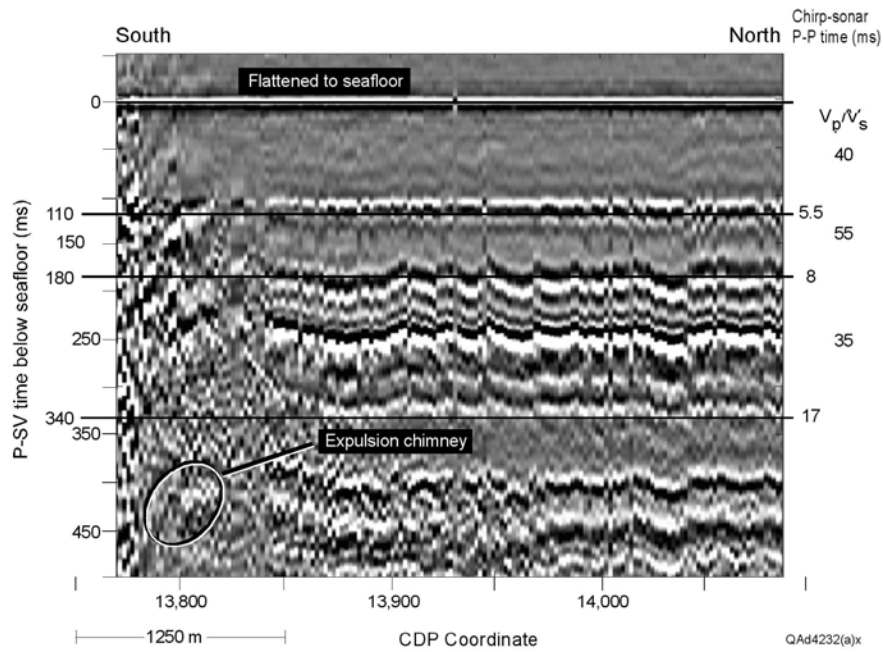


Figure 10. The same images as in Figure 9 with depth-equivalent horizons defined. A P-SV horizon equivalent to the AUV horizon at 2 ms is not labeled because the P-SV reflection event is quite faint in this P-SV display format. Interval values of  $V_p/V_s$  velocity ratio between the P-SV horizons are labeled on the right margins. P-P and P-SV image times are labeled on opposing sides of the images.

## Conclusions

Important software needed for ongoing research at the hydrate monitoring station has been developed and tested using data similar to that expected to be acquired across Block MC 118. This software took long-standing VSP data-processing principles and applied them to deep-water 4C OBC data to create images of deep-water hydrate systems. Test results indicate the software that has been developed is robust and creates higher-resolution P-P images of near-seafloor geology than what can be provided by commercial contractors. Applying VSP-style imaging concepts to deep-water multicomponent seismic data is proving to be invaluable for gas hydrate studies, geomechanical evaluations of deep-water seafloors, and other applications where it is critical to image near-seafloor geology with optimal resolution. However, every seismic data-processing technique has constraints and pitfalls. Two principal constraints of the VSP-based technology described here are:

1. There has to be a significant difference between the elevations of sources and receivers. The technique is not appropriate for multicomponent seismic data acquired in shallow water.
2. The improvement in image resolution over that of production processing of marine multicomponent seismic data diminishes as the image space extends farther (deeper) from the receivers. At significant sub-seafloor depths, production-style, wave-equation-datuming-based, P-P imaging (Fig. 3a) is equivalent or superior to the VSP-style imaging described here.

## References

- Backus, M. M., Murray, P. E., Hardage, B. A., and Graebner, R. J., 2006, High-resolution multicomponent seismic imaging of deep-water gas-hydrate systems: The Leading Edge, v. 25, p. 578 – 596.
- Hardage, B. A., and Murray, P. E., 2006a, High resolution P-P imaging of deepwater near-seafloor geology, AAPG Explorer, v. 27, no. 7, p. 30.
- Hardage, B. A., and Murray, P. E., 2006b, P-SV data most impressive image: AAPG Explorer, v. 27, no. 8, p. 30.

## Abbreviations and Acronyms

**4-C:** four-component

**OBC:** ocean-bottom cable

**P-P:** standard P-wave seismic data

**P-SV:** converted-shear mode (P-wave to SV-shear wave conversion)

**VSP:** vertical seismic profile

**V<sub>P</sub>:** P-wave velocity



# **Coupling of Continuous Geochemical and Sea-floor Acoustic Measurements**

**Progress report for the period  
October 1, 2006 – March 31, 2007**

**April 27, 2007**

*Jeffrey Chanton<sup>1</sup> and Laura Lapham<sup>2</sup>*

<sup>1</sup> *Department of Oceanography, Florida State University, Tallahassee, FL*

<sup>2</sup> *Department of Marine Sciences, University of North Carolina, Chapel Hill, NC*

**Abstract:**

In May 2005, the Pore-Fluid Array (PFA) was installed on the northern flank of Mississippi Canyon 118. The PFA housed four OsmoSamplers within a sampler box that collects pore-fluids slowly over time in order to monitor the *in situ* methane concentrations and other dissolved constituents. In September 2006, the sampler box was retrieved with the submersible Johnson-SeaLink and the pore-fluids were analyzed for chloride and methane concentrations and stable carbon isotopic ratios. Analysis showed that the northern flank of MC 118 is characterized by brine and methane-rich fluids. Since brine inhibits hydrate formation, the discovery of brine radically changes the hydrate stability zone in the northern region of MC 118. The sampler box was also replaced with a new box, ready to collect another time-series of pore-fluid samples. On this same cruise, two other instrument types were deployed in the shallow sediments (<50 cm deep). Pore-water equilibration instruments (peepers) and an OsmoLander were also emplaced directly adjacent to outcropping hydrate to be retrieved at a later date.

**Background:**

Hydrate stability is a function of *in situ* pressure, temperature, and methane concentration conditions. If these conditions change over time, the stability of hydrates could be adversely affected. Therefore, to assess hydrate stability, each of these conditions must be monitored over time. While pressure and temperature measurements are often made, *in situ* dissolved methane concentrations are not. Furthermore, since hydrates exclude salts upon formation, hydrate formation events may be followed by monitoring temporal changes in dissolved chloride and sulfate concentrations. Therefore, the goal of this research is to monitor hydrate stability by quantifying the *in situ* methane and dissolved salt concentrations within hydrate-bearing sediments over time.

*In situ* methane concentrations are difficult to quantify because dissolved methane readily comes out of solution. Without the use of an *in situ* measurement device (i.e. underwater mass spectrometer), the samples must be collected from the seafloor, contained at *in situ* pressures, brought to the surface, and measured for methane concentrations. Yet, containing samples at *in situ* pressures is not a trivial task. Therefore, the quantification of *in situ* methane concentrations will be attained by testing three different instruments. These instruments are currently being tested on the seafloor and are described below.

- 1. Pore-Fluid Array:** The Pore-Fluid Array (PFA) is made up of an interchangeable instrument package that houses four individual OsmoSamplers (Jannasch et al., 2004), a connector that allows the instrument package to be changed out while minimizing sample disruption, and a 10-meter long probe tip along which 8-filtered ports are evenly spaced (Figure 1). At each port, pore-fluids are slowly pumped up the probe tip, across the connector, and into long length of small-diameter tubing coil using OsmoSampler technology to collect ~4 months data with

week resolution. OsmoSamplers collect pore-fluids slowly over time using an osmotic differential created between a brine and DI-water reservoir within the pumps (Figure 2). Two of the four samplers were plumbed into a high-pressure valve that, when closed on the seafloor, kept the sample from degassing upon ascent through the water column. In May 2005, the PFA was deployed on the northern flank of Mississippi Canyon lease block 118 (MC 118), Gulf of Mexico.

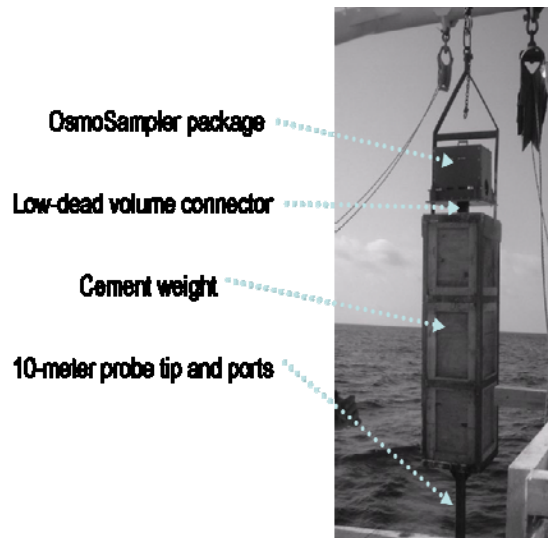


Figure 1: Picture of PFA off back of ship ready for deployment. The four parts that make up the PFA are labeled.

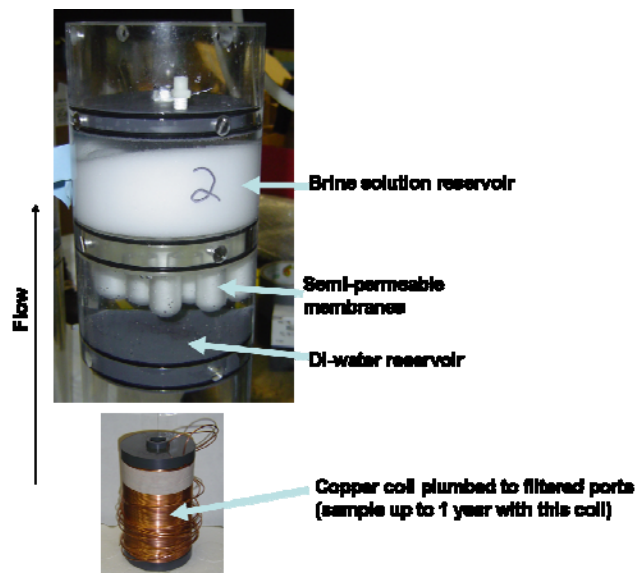


Figure 2: Picture of OsmoSampler and copper tubing spool (Jannasch et al., 1994; Jannasch et al., 2004).

2. **OsmoLander:** Using the OsmoSampler technology, the shallow sediments (upper ~50 cm) were also sampled with a modified PFA called the OsmoLander. The OsmoLander contains four OsmoSampler pumps (similar to the PFA), yet collects pore-fluids directly adjacent to a hydrate surface (Figure 3). Pore-fluids are collected through small tubing housed within a PVC T-handle that is 1, 2, 3, and 4 cm away from the hydrate surface (shown in Figure 2). This instrument contains short length coils to get a snap shot of the *in situ* methane concentration. It also allows for the determination of hydrate dissolution rates to be measured directly.

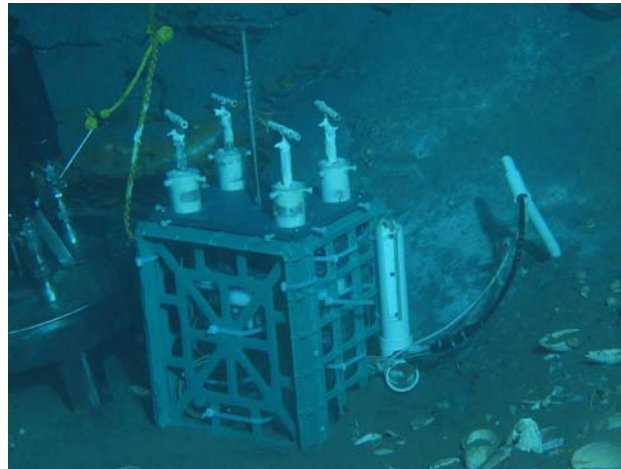
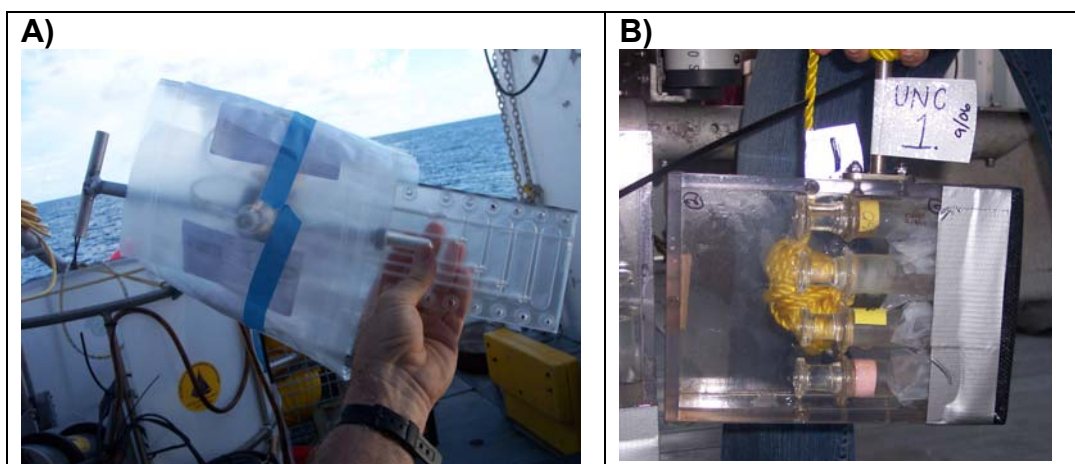


Figure 3: OsmoLander emplaced at MC 118. Four small T-handle valves are visible that will be closed when it is retrieved from the seafloor. To the right of the sampler, the PVC T-handle is visible where samples will be collected.

3. **Peepers:** Pore-water equilibration instruments (peepers) are used to collect fluids, passively, in shallow water systems to measure for dissolved constituents (Hesslein, 1976; Mayer, 1976). Peepers contain several closely spaced sample reservoirs to produce a high-resolution depth profile. The collection is attained by each reservoir being covered by semi-permeable membrane that, when placed in the sediments, equilibrates with dissolved constituents, including gases. However, since typical peepers are used in shallow water systems, they are not affected by changes in pressure when collected and do not contain the samples at *in situ* pressures. Since methane comes readily out of solution, the use of peepers in deep water systems is subjected to pressure issues and may result in the loss of dissolved gases. Therefore, we are testing two modifications to the original peeper design (Figure 4). The first connects plastic bags to each sample reservoir, allowing evolved gases to expand into the bags (Figure 4a). The second design uses cut-off glass syringes whose barrels are allowed to move during gas expansion (Figure 4b).



**Figure 4: Photographs of modified peepers. A) Bagged peeper with sample reservoirs. B) Syringe peeper prior to deployment.**

### **Results of research activities:**

#### **PFA results:**

After 1.5 years, the PFA's instrument package was recovered successfully and the individual OsmoSamplers were found to be collecting from the overlying water, 1.2 m, 3.2 m, and 8.5 meters below the seafloor (mbsf; Figure 5).

From the sampler coils, pore-fluids were extracted and measured for chloride, sulfate, and methane concentrations and methane isotope ratios. The overall results showed normal seawater conditions in the overlying waters, averaging 549 mM chloride (Figure 6a) and 30 mM sulfate (Figure 7). At 8.5 mbsf, chloride concentrations averaged 4600 mM (Figure 6b); strongly suggesting the intrusion of brine fluids. Brine was further indicated by the absence of sulfate, 0.7 mM sulfate (Figure 7). As expected with brine fluids, they were also characterized by high methane concentrations, averaging 4.2 mM with a maximum of 14 mM (Figure 8).

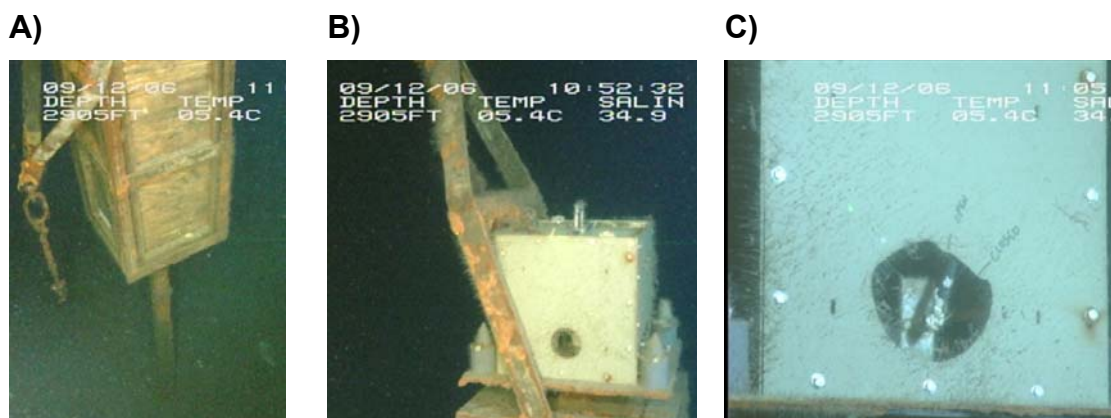
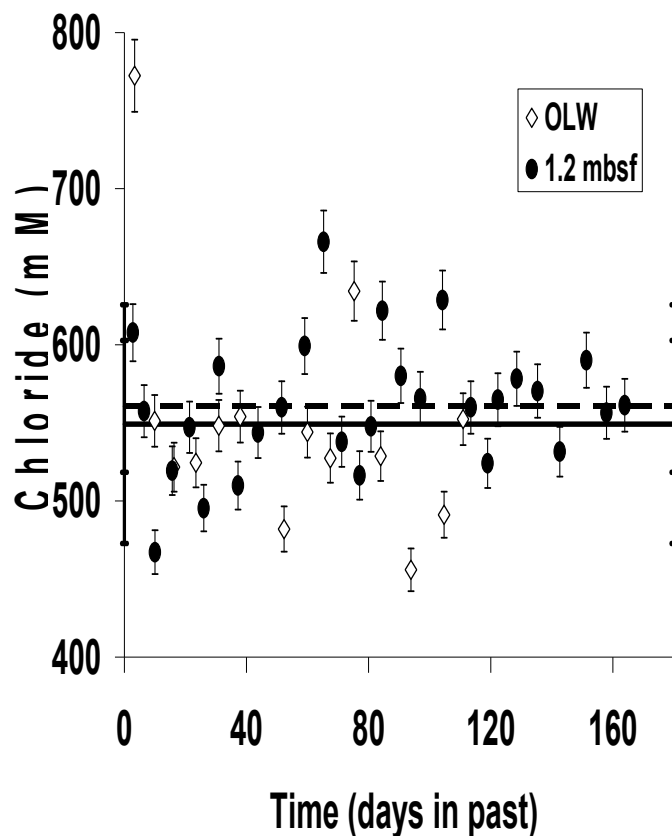


**Figure 5: Seafloor photos of the PFA retrieval. A) The first sighting of the PFA showed it was standing upright and vertical about 2 meters out of the sediment. B) The OsmoSampler package shown with minimal biofouling and all parts intact. C) Although a little corroded, the high pressure valve was still intact.**

A)



B)

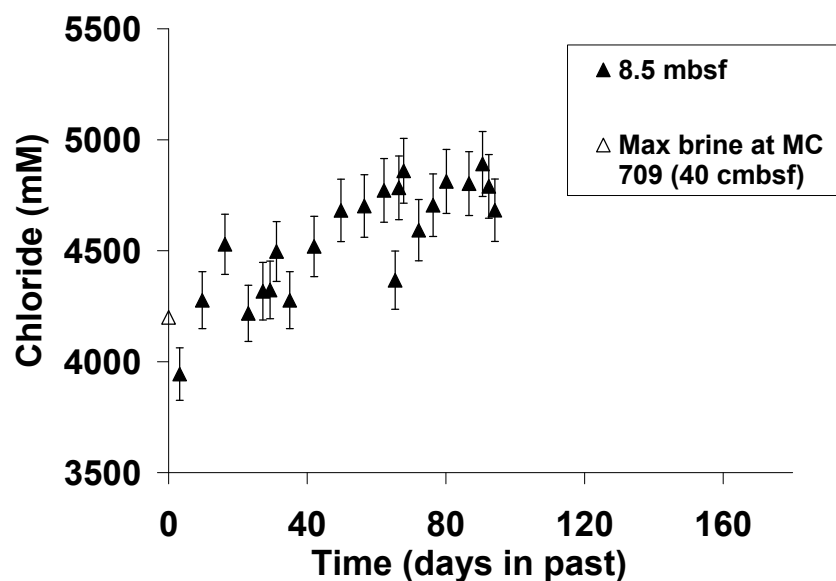


Figure 6: A) Chloride concentrations for overlying water (OLW) and 1.2 mbsf. The dashed and solid lines correspond to the overall average concentrations and standard deviations for 1.2mbsf and OLW samples. B) Chloride concentrations for 8.6 mbsf are plotted in black filled triangles. The open triangle is the chloride concentration measured at a nearby brine field, MC 709. Note the y-axis scale change between A and B. On each point, error bars represent 3% analytical error.

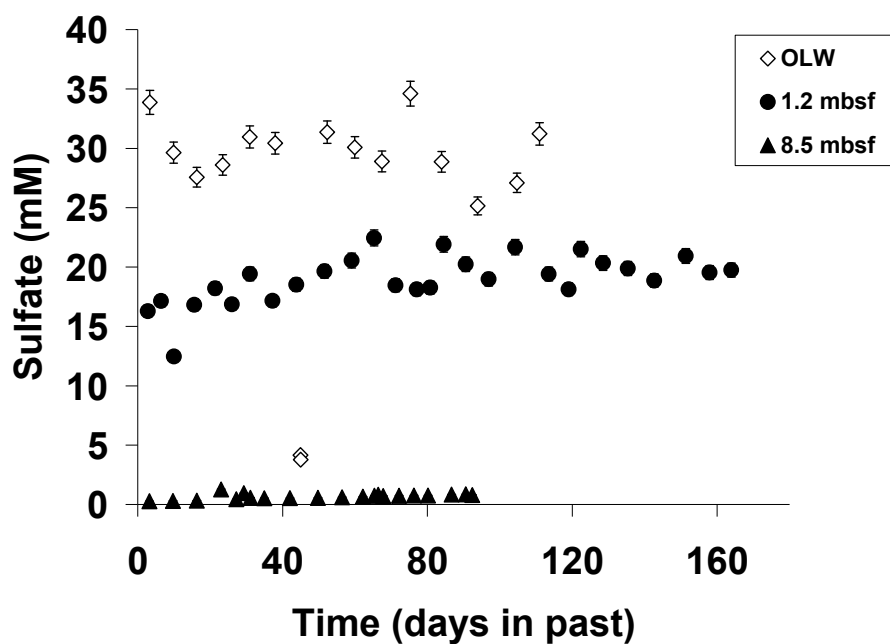


Figure 7: Sulfate concentrations for all three coils measured. On each point, error bars represent 3% analytical error.

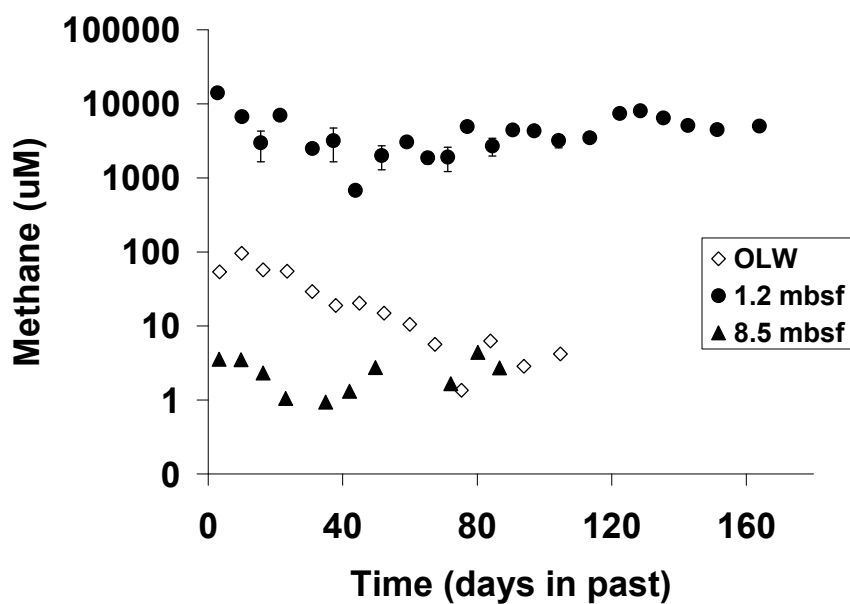
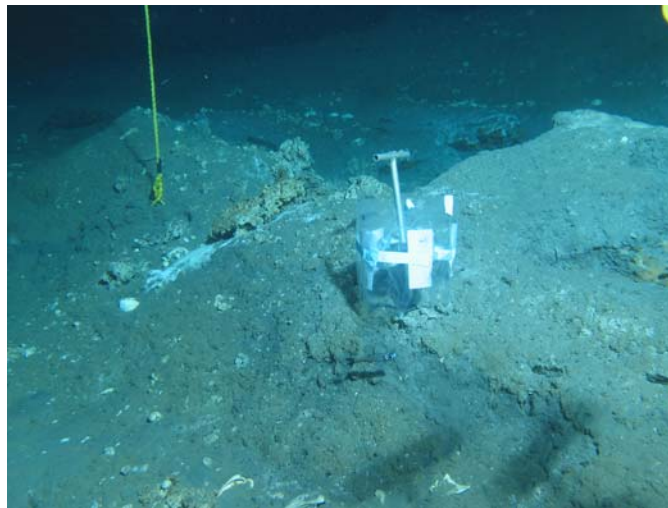


Figure 8: Methane concentrations for all three coils measured. Note log scale y-axis.

**Emplacement of sea-floor instruments:** In September 2006, six modified peepers were emplaced at MC 118 at three different sites (Table 1 and Figure 9). These instruments will be picked up in future cruises.

**Table 1: Summary of seafloor instruments emplaced at MC 118.**

Site	# of Bagged Peepers	# of Syringe Peepers
Mandyville	1	0
Rudyville	2	2
Noakesville	1	0



**Figure 99: Sea-floor photograph of a bagged peeper at Mandyville. The yellow vertical line off to the left of the picture is marker #1.**

---

### **Publications:**

Lapham L. L. (2007) *In situ* measurements of methane cycling in cold seep sediments containing gas hydrates and brines. Ph.D., University of North Carolina.

### **Presentations:**

Lapham, L. L., J. P. Chanton, C. S. Martens, P. D. Higley, H. W. Jannasch, J. R. Woolsey, and K. Sleeper. 2007. Biogeochemical sensors: design and applications of the Pore Fluid Array for the Mississippi Canyon 118 Gas Hydrate Seafloor Observatory. Oral presentation by Ken Sleeper, Mid-South Area Engineering and Sciences Conference, University of Mississippi. Oxford, MS May 17-18.



Lapham, L. L., J. P. Chanton, C. S. Martens, P. D. Higley, H. W. Jannasch and J. R. Woolsey. 2007. Monitoring long term hydrate stability: *in situ* methane and the Pore Fluid Array (PFA). Oral presentation, Gulf of Mexico Hydrates Research Consortium Annual Meeting. Oxford, MS.

#### References cited:

- Hesslein R. H. (1976) An *in situ* sampler for close interval pore water studies. *Limnology and Oceanography* **21**, 912-914.
- Jannasch H. W., Johnson K. S., and Sakamoto C. M. (1994) Submersible, osmotically pumped analyzers for continuous determination of nitrate *in situ*. *Analytical Chemistry* **66**, 3352-3361.
- Jannasch H. W., Wheat C. G., Plant J. N., Kastner M., and Stakes D. S. (2004) Continuous chemical monitoring with osmotically pumped water samplers: OsmoSampler design and applications. *Limnology and Oceanography: Methods* **2**, 102-113.
- Mayer L. (1976) Chemical water sampling in lakes and sediments with dialysis bags. *Limnology and Oceanography* **21** (6), 909-912.
- Sassen R., Roberts H. H., Jung W., Lutken C. B., DeFreitas D. A., Sweet S. T., and Guinasso Jr. N. L. (2006) The Mississippi Canyon 118 Gas Hydrate Site: A complex natural system. *OTC Paper #18132; Offshore Technology Conference*.

# **Microbial Activity Related to Gas Hydrate Formation and Seafloor Instabilities**

## **FINAL REPORT**

**R.E. Rogers: Principal Investigator  
G. Zhang, J. Dearman, S. Xiong  
Swalm School of Chemical Engineering  
Mississippi State University**

**May 17, 2007**

## **ABSTRACT**

This final report covers the contract work beginning 1 January 2005 and concluding 1 January 2007.

Location and extent of seafloor hydrate occurrences are influenced by mineral content, microbial activity, fluid properties and physical properties of the sediments and by the hydrocarbon gas flux through the sediments. The goal of the research was to provide data to help establish mechanisms of seafloor hydrate formations and to provide guidelines to eventually locate hydrate deposits suitable for gas production. The work supported the planning and installation of the Gas Hydrate Observatory.

Numerous sediments from Mississippi Canyon blocks MC-118 and MC-798 were analyzed in the laboratory for influence on forming gas hydrates. Hydrate formation rates and crystal initiation times in a series of cores were measured in the laboratory as a function of depth below seafloor and as a function of lateral displacement at the seafloor surface. Results suggest sulfate zone depth, bioactivity, pore-water salinity, mineral content, bioproducts coating sediment particles, and sediment particle sizes impact hydrate nucleation and formation in near-surface sediments.

A core to 30 mbsf from the Dufresne cruise at MC-798 provided a unique evaluation of deep hydrate formations in Gulf of Mexico sediments that could be compared to numerous cores of less than 6 mbsf depths from the Mississippi Canyon.

The laboratory results show sediments below the sulfate zone to more easily form hydrates. Near-surface sediments showed random effects on gas hydrate formation believed caused by different sets of bioproducts coating mineral surfaces in the sulfate zone. The depth of the sulfate zone is highly dependent upon methane flux through the sediments.

Basic smectite clay platelets were again verified to act as hydrate nucleation sites.

Five significant publications derived from the grant. One PhD dissertation research and degree accrued from the grant.

## **I. INTRODUCTION**

### **A. Gas Hydrate Occurrence and Microbial Influences in Hydrate Zones**

Most analyses of gas hydrates in the GOM have been done on the top 6 meters of sediments (Milkov and Sassen, 2000), although the bottom of the gas hydrate zone in the Gulf of Mexico might extend 200- 1000 m (Milkov and Sassen, 2002). The Dufresne core MD02-2570 takes on added importance because it extends to depths of about 30 meters and allows the study of hydrate formation in sediments deeper than usual.

Microbial activity in the Gulf of Mexico around gas hydrate occurrences is prolific (Roberts, 2004; Sassen et al., 2001). For lack of research, it has been

too easy to assume that extensive microbial occurrences near massive hydrate mounds are coincidental. The association is probably much more complex than just biogenic gases being supplied as guest gases for hydrates. Microbes insert abundant lipids into the hydrate –bearing sediments that may promote hydrates; these hydrates prefer the proximity of complex microbial consortia and chemosynthetic communities (Sassen et al., 1999).

In the Cascadia Margin, bacterial populations and activity were found to increase by about an order of magnitude throughout gas hydrate zones wherever hydrates occurred, except in places of high H<sub>2</sub>S concentration (Cragg et al., 1996).

## **B. Laboratory Study of Bioagents and Gas Hydrate Relationships**

When bacteria produce surfactants, the surface-active agent falls into one of five classifications: (1) hydroxylated and crosslinked fatty acids, (2) polysaccharide-lipid complexes, (3) glycolipids, (4) lipoprotein-lipopeptides, or (5) phospholipids (Kosaric, 1992; Fujii, 1998).

To test the hypothesis that biosurfactants could catalyze hydrate formation, a sample of at least one biosurfactant from each classification was obtained from commercial sources. The results were emphatic. These biosurfactants catalyzed hydrate formation in packed porous media (Rogers et al., 2003). The following effects of biosurfactants in the porous media were observed: (1) Hydrate formation rates were usually increased. (2) Hydrate induction times were usually decreased. (3) Specific mineral surface-biosurfactant interactions developed. (4) Very low threshold concentrations of biosurfactants were required to catalyze hydrates.

Porous media of sand and sodium montmorillonite packed in a laboratory test cell and saturated with seawater containing 1000 ppm of biosurfactant showed a two to four-fold increase in hydrate formation rate over a control of the same media saturated with seawater without surfactant. Of the biosurfactants tested, surfactin is classified a lipopeptide, and snomax and emulsan are polysaccharide-lipid complexes.

It is helpful to remember approximate depths of the hydrate zone as compared to the depth of near-surface cores being analyzed. Typically, the hydrate zone depth would be about 200 mbsf in the Mississippi Canyon, whereas the Dufresne cores extended to 30 mbsf and available push cores reach to about 6 mbsf. In fact, most of the limited hydrate-formation data reported in the literature for GOM.

## **II. THEORY**

### **A. Hypothesized Mechanism Affecting Near-Surface Hydrate Formation**

Sulfate from the overhead seawater permeates the near-surface sediments and comes to equilibrium in this sulfate zone. Anaerobic oxidation of

methane occurs in the sulfate zone. Archaea clusters work in consort with sulfate-reducing bacteria. The bacteria reduce sulfate to  $\text{H}_2\text{S}$ , and archaea concurrently oxidize methane to form  $\text{CO}_2$ . The  $\text{CO}_2$  precipitates as carbonates at the point of anaerobic methane oxidation. As the upward methane flux increases through the sediments, the sulfate zone ascends to nearer the sediment-sea interface. For example, the bottom of the sulfate zone has been reported to be only a few centimeters deep near gas hydrate outcrops and methane gas vents. Carbonate nodules solidify and become an indicator of the current bottom of the sulfate zone or a previous sulfate boundary.

Bioproducts from the microbes in the sulfate zone differ from those below the sulfate zone, and the catalytic effects of those bioproducts on hydrate formation could be expected to differ. (The catalytic effect of bioproducts probably depends on whether there are distinct hydrophobic and hydrophilic components in the same molecular structure. The hydrophobic moieties collect the methane and the nearby hydrophilic moieties collect and structure water, thus setting up the nuclei for hydrate initiation. Anionic bioagents and anionic synthetic agents have proven to be hydrate catalysts.) The sediment particles in the sulfate zone may be covered with polymeric bioproducts that do not have distinguishing hydrophilic and hydrophobic components, contrasting to those below the sulfate zone. A nonionic polymeric coating of near-surface mineral particles could slow or prevent local hydrate formation.

If this hypothesis is used to help interpret the hydrate formation and induction curves generated in the laboratory from MC-118 sediments, then from generated curves one might determine the location of the sulfate zone and have a good indicator of the magnitude of the methane flux at that location.

### **III. EXPERIMENTAL PROCEDURE**

#### **A. Procedure for Analyzing Dufresne Cores**

Sediment samples were taken from the approximately 30 m long core extracted from 28°04.26'N and 89°41.39'W in the Gulf of Mexico during the Marion Dufresne cruise. Generally, laboratory samples were chosen at 3-meter core intervals. The mud samples were immediately sealed in Zip-lock plastic bags and stored in air-conditioned rooms until tested.

To prepare samples for testing, constant 20 g weights of sediment were taken from each interval and dispersed in a constant 60 g weight of cleaned sand to provide adequate permeability and porosity of the packed media so that maximum surface area of sediments in each experimental run would be exposed to pressurizing hydrocarbon gas in the test cell. For tests, original pore waters saturated the porous media; no other water was added to the samples. For testing, the 60/20 sand/sediment mixtures were placed in a 60 ml Teflon

container with twelve 1/8 in. holes drilled in the container walls for gas access. The sample container was placed in a 400 ml stainless steel test cell from Parr Instrument Company. An RTD resistance temperature detector was positioned just below the sand/sediment surface. A pressure transducer measured internal pressure of the reaction vessel. The cell was purged of air and then pressurized with natural gas (90% methane, 6% ethane, 4% propane) to 330 psig. After the system had equilibrated at 70°F in a constant temperature bath for two hours, pressure was adjusted to 320 psig and the system allowed to equilibrate for another hour. Then, the test cell was immersed in a constant-temperature bath at 0.5°C and data collected every 2 minutes with Omega Daqbook 120 equipped with DBK9 Data Acquisition System and DasyLab Software. Pressure versus temperature was plotted.

Induction time of the hydrates was defined as elapsed time between the calculated equilibrium pressure-temperature and the observed hydrate formation during system cool-down. The induction time was standardized by dividing by the induction time for the sediment test sample of 1.0 m depth.

Hydrate formation rate, as the number of moles of gas going into solid solution per unit time, was determined with the Peng-Robinson equation of state from data collected in 2-minute intervals. To standardize, maximum formation rate was divided by the maximum formation rate for the 1 m sediment control. Duplicate runs were made on each sample.

## **B. Analyzing Near-Surface Cores**

Important features of the laboratory procedure for analyzing near-surface cores are listed below.

1. Twenty grams of mud samples are evenly dispersed through 60 grams of coarse Ottawa sand that has been cleaned. The reasons for doing this are the following: (a) to give maximum access of natural gas to the sediment samples, thus exposing maximum surface areas of the sediment particles to the reacting gas, (b) to provide larger porosities in which hydrates are allowed to form and expand, (c) to be able to utilize the small mud sample sizes.
2. The samples are tested for hydrate formation in Teflon containers. Teflon provides a hydrophobic surface that does not affect hydrate formation.
3. For testing, the samples are placed in annular spaces of concentric Teflon cylinders. Both cylinders have many gas-access holes spaced over their entire areas. This allows maximum contact of gas with sediments and prevents mass transfer from limiting hydrate kinetics.
4. Only original seawater removed with the cores is present in the tests.
5. Teflon containers with samples are placed in stainless steel Parr reactors, sealed, pressurized with natural gas and submerged in constant temperature baths maintained at 0.5°C.
6. Pressures and temperatures are recorded continuously during the tests.

## IV. RESULTS AND DISCUSSION

### A. Hydrate Formation Rate Variation with Depth

The Marion Dufresne MD02-2570 cores extracted from 0- 30 mbsf (meters below seafloor) provide an opportunity to study hydrate formation in sediments below the 6 m commonly tested in the Gulf of Mexico. The approach was to evaluate sediments from the surface to the 30 m bottom in 3 m intervals.

The laboratory hydrate tests repeated the following conditions: (1) Only original in-situ pore water saturated sediment test samples. (2) Each sediment sample was dispersed in cleaned Ottawa sand to give adequate porosity and permeability for testing. (3) Sediment dispersion throughout the sand gave maximum contact of minerals with natural gas. (4) Natural gas of 90% methane, 6% ethane, and 4% propane pressurized the hydrate test cell.

Resulting gas-hydrate formation rates are given in Table I and plotted in Figure 1. Each tabulated value is an average of duplicate, multiple, independent runs.

**TABLE I.** Gas-hydrate formation rates of sediments from Dufresne MD02-2570

Depth, meters	Formation Rate, mmol/hr	Standardized Form. Rate
0.00	0.00 Did not form	0.00
1.00	5.26	1.00
3.00	20.37	3.87
6.00	22.02	4.19
9.00	26.32	5.00
12.00	27.06	5.14
15.00	39.02	7.42
18.00	37.15	7.06
21.00	35.13	6.68
24.00	27.79	5.28
27.00	24.87	4.73
27+ (Plotted as 30 m)	23.96	4.56

An apparent trend in the gas-hydrate formation rates as a function of distance below sea floor (mbsf) can be detected in Fig. 1. Hydrates would not form in the nearest-surface sediments--even after sustaining hydrate-forming conditions for 96.5 hours. (This zero-depth test was terminated at 96.5 hours.) As depths increased, however, hydrate formation rates in the sediment samples increased until a maximum occurred for the mud at 15-20 mbsf.

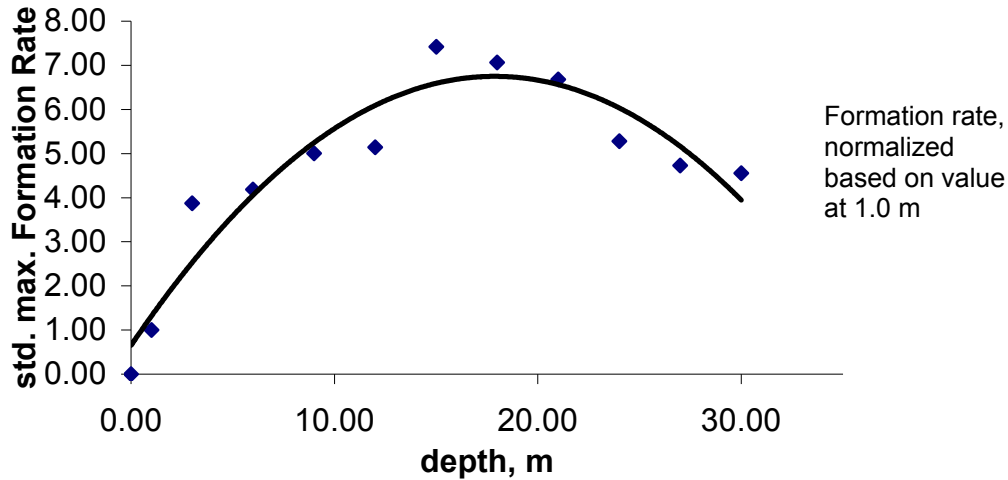


**Fig. 1.** Evaluation of core sediments for rate of hydrate formation

The correlation of hydrate formation rate with depth in Figure 1 may be represented by the regression Equation (1).

$$FR = -0.0191 D^2 + 0.6823 D + 0.6512 \quad (1)$$

In the equation FR is the standardized maximum formation rate, D is the depth of sediments as meters. The  $R^2$  for the correlation is 0.9034.

## **B. Hydrate Induction Time Variation with Depth**

Sediment samples from Dufresne MD02-2570 were generally tested every 3.00 meters. Exceptions were a surface sample and a sample 1.00 meters below the surface. In the context of hydrocarbon gas migrating through seafloor sediments, induction time might be considered an indication of the gas residence time necessary to initiate hydrates. Therefore, induction time may be taken as one indication of the propensity for hydrate occurrence.

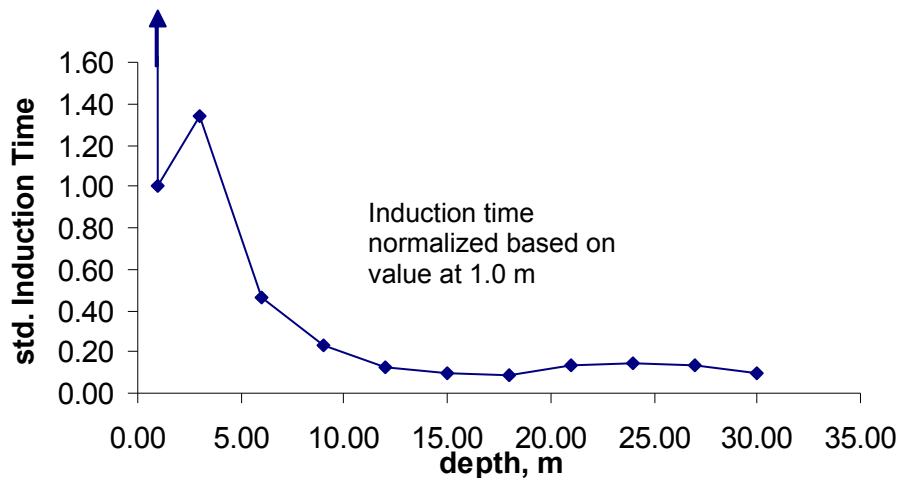
In Table II are the gas hydrate induction times for each sample depth; each data point represents an average of multiple runs. A standardized, dimensionless time is calculated by taking the induction time of the 1.00 sample as the reference. In the case of the surface sample, note that gas hydrates had not formed after 95.6 hours under hydrate conditions.



**TABLE II.** Gas-hydrate induction times of sediments from Well MD02-2570

Depth, meters	Induction Time, hr	Standardized Induction Time
0.00	Did not form.	$\infty$
1.00	4.33	1.00
3.00	5.82	1.34
6.00	2.00	0.46
9.00	1.00	0.23
12.00	0.53	0.12
15.00	0.42	0.10
18.00	0.37	0.08
21.00	0.60	0.14
24.00	0.63	0.15
27.00	0.58	0.13
27+ (Plotted as 30 m)	0.43	0.10

The induction time-depth trend is more readily envisioned with the help of Figure 2.

**Fig. 2.** Hydrate induction times for the Dufresne core.

A rapid decrease in induction time, i.e., an improvement in the ease with which hydrates initially form, is evident down to an approximate 12 m depth. There, the induction time reaches a minimum and remains at that rapid initiation for the remainder of the 30 m.

In the top few meters of near-surface sediments, the trend is disrupted.

It is helpful to superpose the induction time and formation rate curves in Figure 3, where the two phenomena are compared.

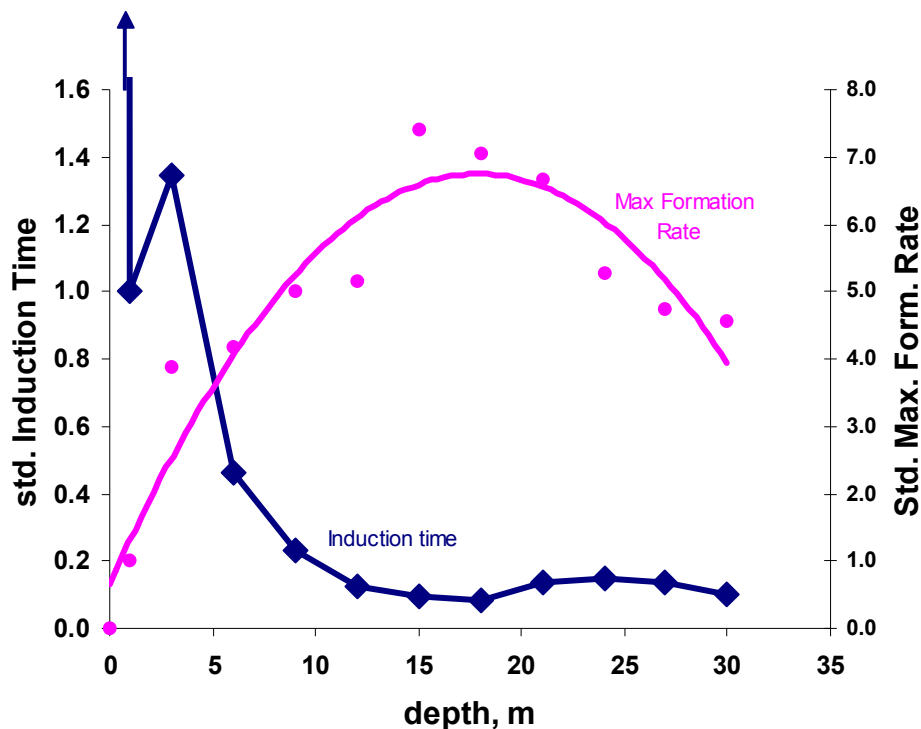


**Fig. 3.** Relative formation rates and induction times of gas hydrates

Induction time, the rapidity of hydrate initiation, primarily depends upon density and quality of nucleation sites. General studies in our laboratory of hydrate formation in sediments suggest the importance of smectite clay particles and the presence of bioproducts that may adsorb on those small clay particles as promoting short hydrate induction times, although apparently there are other influences on induction time that remain an enigma. The bioproducts bring hydrocarbon gas and structured water together at the nucleation site, as compared to their random meeting, thus reducing induction time.

After hydrate initiation, the rate of hydrate particle agglomeration must obviously depend on mass (hydrocarbon gas as well as water) transfer rate, heat transfer rate, surface area on which hydrates form, porosity for hydrate growth, temperature, pressure, bioproducts, and mineral surfaces—an imposing array of variables. Consider mass transfer rates, heat transfer rates, temperatures, and pressures constant in these experiments.

From the Dufresne MD02-2570 data, it is concluded from Figure 3 that hydrates occur in the sediments with varying difficulties and rates as a function of depth below the seafloor.

### C. Silt, Clay, Sand Compositional Change with Depth

Sand, silt, and clay contents were analyzed for each of the samples of the 30 m core extracted during the Dufresne cruise.

In order to compare results directly with the hydrate formation rate and induction time trends, the sand/silt/clay contents were normalized and plotted versus depth in Figure 4.

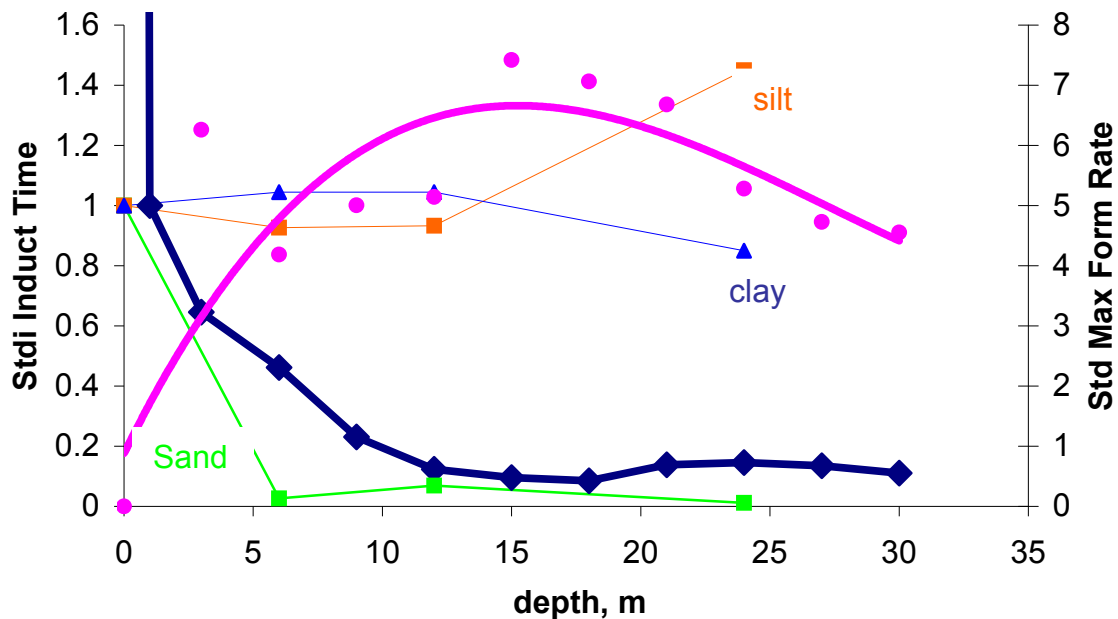


Fig. 4. Sand/silt/clay contents

It is interesting that breaks in the trends of sand/silt/clay roughly occur near where the breaks develop in induction time and formation rate trends. Although no definitive conclusion can be drawn from this limited number of data points, the relative trends suggest future verification in other cores and suggest tangential experiments that will be undertaken.

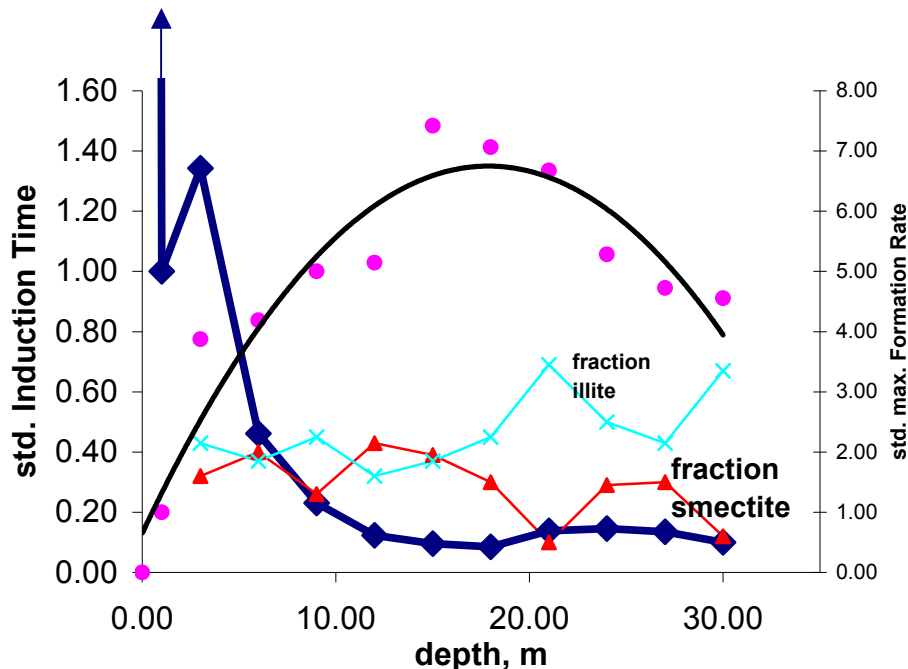
### D. Clay Content of Dufresne Sediments with Depth

Clay minerals in each sediment sample of the Dufresne core were analyzed with depth and the percentage compositions are presented in Table III. These data represent compositions of particles  $\leq 2 \mu\text{m}$  diameter.

**TABLE III.** Clay content of MD 02 2570

Depth (m)	% smectite	% illite	%chlorite	% kaolinite
3	32	43	8	18
6	40	37	6	18
9	26	45	6	23
12	43	32	5	20
15	39	37	7	17
18	30	45	6	20
21	10	69	10	11
24	29	50	9	12
27	30	43	8	19
27.1	12	67	10	11

In Table III it is seen that kaolinite and chlorite represent a lower fraction of clay content, and the percentages of these two minerals remain fairly constant with depth. It therefore seems more important to concentrate on the smectite and illite contents, so these clay contents are plotted versus depth in Figure 5.

**Fig. 5.** Predominant clay content of sediments; <2 micron diameter particles

#### E. Sediment Particle Sizes with Depth

The Dufresne MD02-2570 cores are especially useful because they extend to about 30 mbsf, much deeper than any other available cores.

Particle size distributions were obtained for the MD02-2570 sediments for three depths: 1.5, 9.0, and 27.0 mbsf. The analyses were conducted with a Malvern MasterSizer Laser diffractor instrument. The instrument determines particle

volume distribution from laser diffraction patterns of a cloud of the particles, and the data are presented on the basis of an equivalent spherical diameter. The instrument evaluates size ranges from 0.02  $\mu\text{m}$  to 2000  $\mu\text{m}$ . From the measurements, specific surface areas, surface weighted mean diameters and volume-weighted-mean diameters are presented in Table IV.

**TABLE IV.** Particle sizes of MD02-2570 sediments

Sample depth, m	Specific surface area, $\text{m}^2/\text{g}$	Surface weighted mean dia, $\mu\text{m}$	Volume weighted mean dia, $\mu\text{m}$
1.5	3.04	1.974	7.680
9.0	2.92	2.056	9.003
27.0	2.43	2.472	7.206

It is evident in Table IV that mean particle diameter generally increases with depth. Comparison of volume-weighted mean diameters with surface-weighted mean diameters, show a difference in size distributions with depth that suggest a large number of small particles in the sediments.

Smaller particles should decrease induction time by providing numerous nucleation sites. The smaller particles would also more likely be coated with bioproducts that could increase or decrease induction time depending on the bioproduct composition. Furthermore, bioproducts vary with depth. For example, near the seafloor sulfate-reducing bacteria act in consort with methane oxidizing archaea as the dominant microbial action. Below the sulfate zone, a different microbial activity and consortia exists.

The larger particles may influence hydrate formation rate because of providing a larger porosity of the porous media in which the hydrates can expand. The large particle size distribution observed in these analyses seemed to substantiate the trend of hydrate formation rates with depth in the MD02-2570 sediments, where rates peaked near 10- 20 m depth, as detailed in earlier reports.

#### **F. Near-Surface Sediments of MC-118**

(1) *Core 11, MC-118.* Formation rates and induction times determined in laboratory measurements of Gulf of Mexico (GOM) sediments (Dufresne MD02-2570 cores) show distinct trends to 30-m depths. The results are now compared to shallower cores from different locations in the Mississippi Canyon.

Generally, when induction times decrease, hydrates begin forming more quickly. This can be important when gases percolate through sediments and have a

limited residence time. After the hydrates are initiated, higher formation rates favor hydrate accumulations in the sediments.

Presented in Fig. 6 are formation rates/induction times of laboratory hydrates developing in the indigenous water-saturated sediments of MC118, Core 11. The patterns of formation rate and induction time in Fig. 6 are somewhat atypical patterns in that induction times increase at about 200 cm depth.

In interpreting the data, the atypical behavior could mean that the bottom of the sulfate zone has not been reached at 297.5 cm—the deepest sample from Core 11. If so, this would mean a relatively low methane flux through the sediments. It could also suggest turbulent mixing of top sediments. In the laboratory, anionic bioagents increase the formation rates of hydrates and decrease the induction times of hydrates. Since different microbial communities exist above and below the sulfate zone, each community would be associated with a unique bioproduct. These bioproducts may have significantly different effects on gas-hydrate formation.

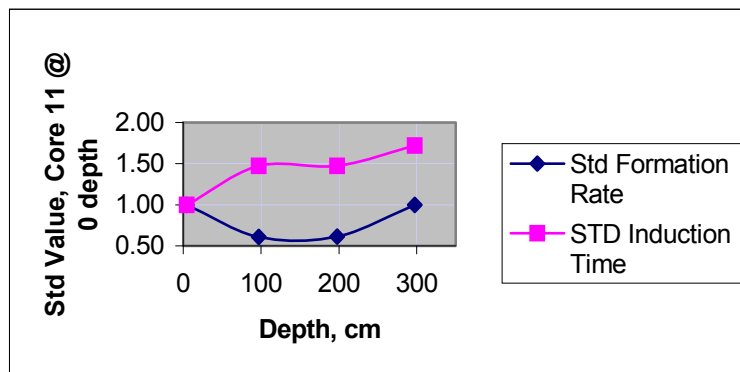


Fig. 6. Hydrate formation in Core 11 from MC-118

(2) *Core 04, MC798*. In Fig. 7, analysis of sediment from MC798, Core 04, gives a more typical pattern of induction time decrease with depth similar to that observed in the deep Dufresne core.

Possibly, the bottom of the sulfate zone could be within a few centimeters of the surface; this would explain patterns of the formation rates and induction times. If so, a relatively high methane flux might pass through the sediments at this core location.

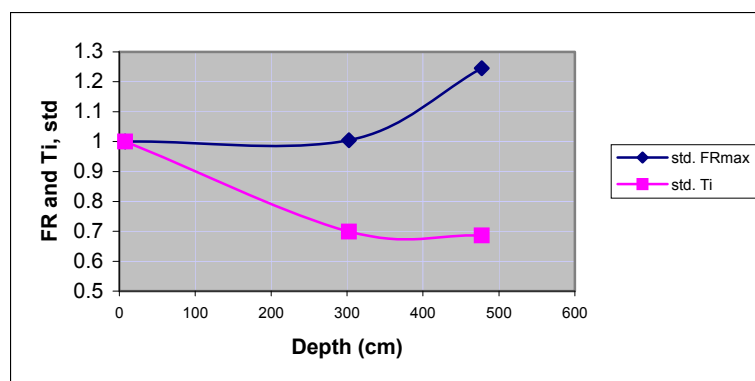


Fig. 7. Hydrate formation in Core 04 from MC-798

The laboratory-generated hydrate curves were interpreted with help from the stratigraphic analyses of Dr. C. Brunner as well as the comments from the core descriptions made during core retrieval.

### G. Patterns of Hydrate Formation with Sediment Depth

*Norm Pattern.* Hydrate formation rates and hydrate induction times differ widely as a function of depth in sediments from near-surface GOM cores. However, patterns demonstrated in Figures 8, 9, and 10 repeat fairly consistently in these three cores composed primarily of homogeneous mud from block MC-798. (The lithostratigraphy was established by Dr. Charlotte Brunner, University of Southern Mississippi, during analysis of sediments from the same core.)

In the three cores, hydrate formation rates increased with depth until a maximum was reached as compared to surface values. The induction times show decreases with depth until a minimum is reached. The patterns are similar to the formation rate and induction time patterns of the deep Dufresne core.

*High Salinity.* Compare Fig. 4 for the Dufresne core with the 'norm pattern' of Figure 8 through Figure 10, where the homogeneous core samples of Figure 8 through 10 are termed the norm. Below 200 cm bsf, it is evident that formation rates decline and induction times increase with depth below the surface.

These formation rates and induction times denote that hydrates are increasingly more difficult to form as depth increases below 200 cm bsf. Dr. Brunner's analyses of samples from the same core found "high pore water salinity 200 cm to bottom of core..." The hydrate tests of these sediments, therefore, seem to verify the known retarding action of saline waters on hydrate formation.

*Sulfate Zone.* It is hypothesized that one of the most important factors in hydrate formation in near-surface sediments is the depth of the sulfate zone. The shallower the sulfate zone depth, the greater is the methane flux through the zone. The microbial communities working in the sulfate zone differ from those below the zone. Bioproducts differ in the zone. Recall that

biopolymers/biosurfactants have been shown in our laboratory to have a significant effect on hydrate formation. Because of the anaerobic oxidation of methane in the sulfate zone and the reduction of sulfate, carbonate nodules as well as hydrogen sulfide occur there.

In Figure 13 (MC 118, Core 29; 28° 51.3293' N and 88° 29.4996' W) are the plots of formation rates and induction times for sediments from Core 29 that reached a depth of 120 cm. In the core description was noted that shells occurred at 21 cm depth. Figure 13 indicates a maximum in both formation rate and induction time at this 21 cm depth. The core description also noted a sulfur smell at 80 cm and 115 cm. Minimums occur in formation rates and induction times at these points.

In Figure 11 (MC 798, Core 05; 28° 4.0000 N and 89° 42.0003 W) are the plots of formation rates and induction times for sediments from Core 05 that reached a depth of 600 cm. Carbonate nodules were observed at 240 and 260 cm. At these depths, Fig. 11 indicates minima and maxima in formation rates and induction times.

Again, in Figure 14 with Core 06, MC 798 (28° 85.3904 N and 89° 39.4997 W) a maximum is reached on hydrate formation rate and a minimum on induction time at the point where fine-grained carbonates occur from a 140 cm to 240 cm depth interval according to Dr. Brunner's lithostratigraphy.

More data are needed for a conclusive interpretation, but these multiple cores indicate some substantial alterations in hydrate-formation propensity at depths where carbonate nodules or sulfur smell (probably H<sub>2</sub>S) occur.

In Figure 12 (MC 118, Core 13, 28° 52.55' N; 88° 28.7' W) is the plot of formation rates and induction times as measured in the laboratory for sediments from Core 13 that reached a depth of 300 cm bsf. In the core description, it was noted that from 56 to 130 cm disseminated shells occurred. The laboratory tests of hydrate formation in these sediments indicated a minimum was reached in both rate and induction time over the depth increment where the disseminated shells occurred. These carbonate nodules may typify the bottom of the sulfate zone, or where the bottom of the sulfate zone was at one time.

## **H. Microbial Activity**

MC 118, Core 12 (28° 52.45' N and 88° 29.2' W) appears as Figure 15. The core description states the depth interval from 20 to 70 cm was bioturbated. The plots of hydrate formation rates and induction times from laboratory data show in this region an increase of formation rate and a decrease in induction time, consistent with the expectation that these particular bioproducts cause the same sort of hydrate promotion as the ones tested in the laboratory.



Similarly, in Cores 08A and 08B of Figure 9 and Figure 10 the laboratory hydrate formation rates and induction times from the sediments show an increase of formation rate and a decrease in induction time over the interval of 200 to 300 cm depth where Dr. Brunner's lithostratigraphy shows microbial action occurring.

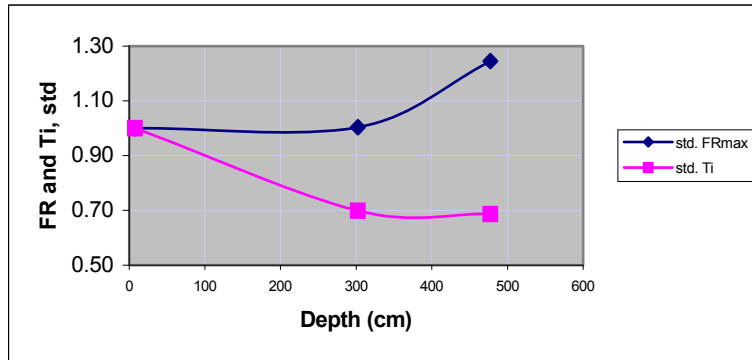


**Fig. 8.** Hydrate formation in Core 04 from MC-798 (28° 8.1176 N, 89° 39.6689 W)

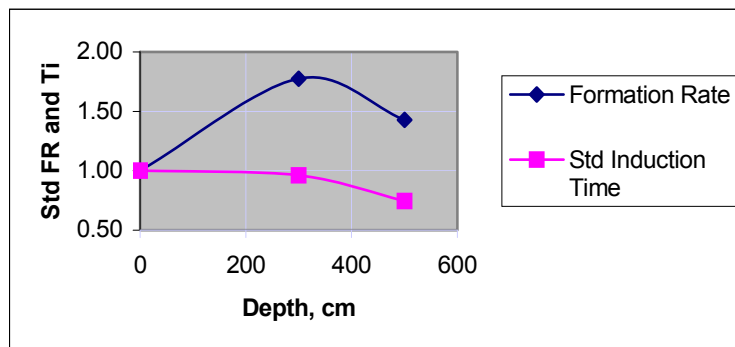


**Fig. 9.** Hydrate formation in Core 08A from MC-798 (28° 2.8914 N, 89° 44.4297 W)

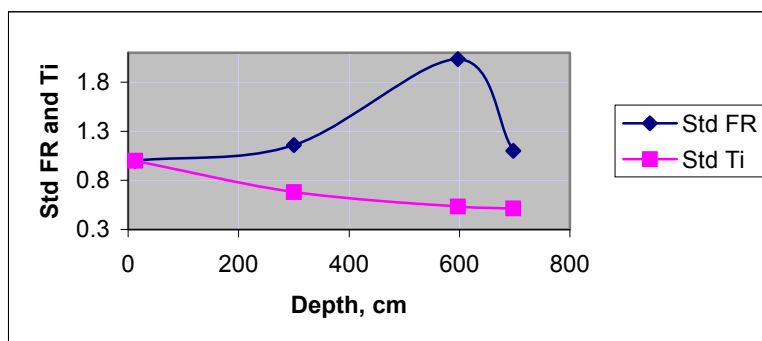


**Fig. 10.** Hydrate formation in Core 08B from MC-798 (28° 2.8183 N, 89° 44.4321 W)

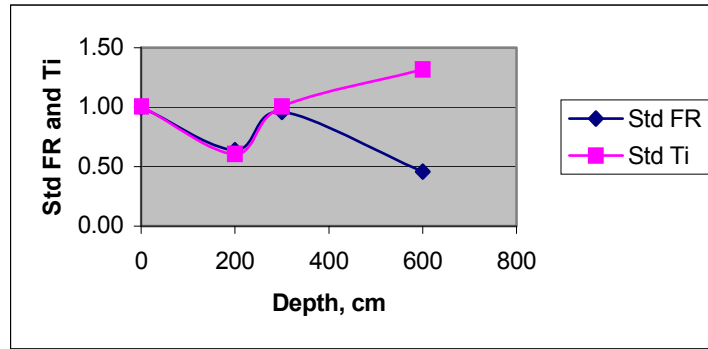


**Fig. 11.** Hydrate formation in Core 05 from MC 798  
( $28^{\circ} 4.0000$  N,  $89^{\circ} 42.0003$  W)

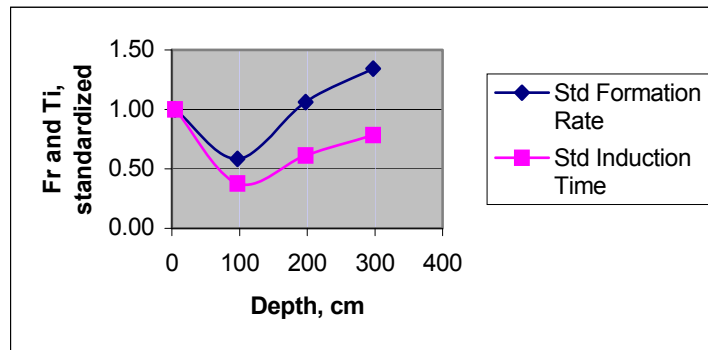


**Fig. 12.** Hydrate formation in Core 13 from MC 118  
( $28^{\circ} 52.55'$  N,  $88^{\circ} 28.7'$  W)

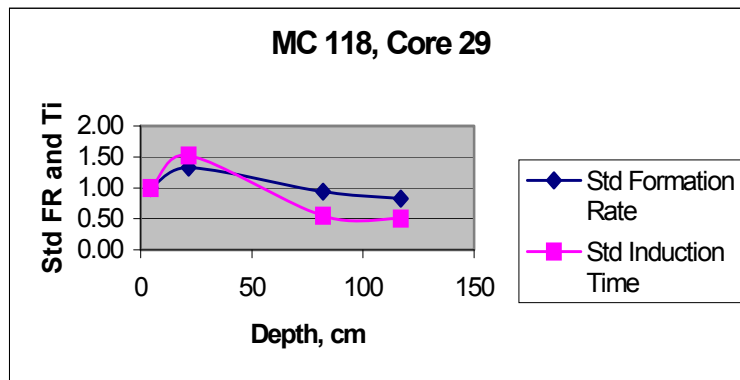


**Fig. 13.** Hydrate formation in Core 29 from MC 118  
( $28^{\circ} 51.3293'$  N and  $88^{\circ} 29.4996'$  W)

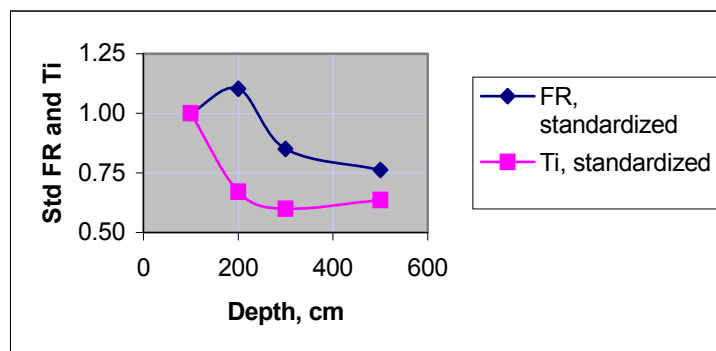


**Fig. 14.** Hydrate formation in Core 06, MC 798 ( $28^{\circ} 85.3904$  N and  $89^{\circ} 39.4997$  W)

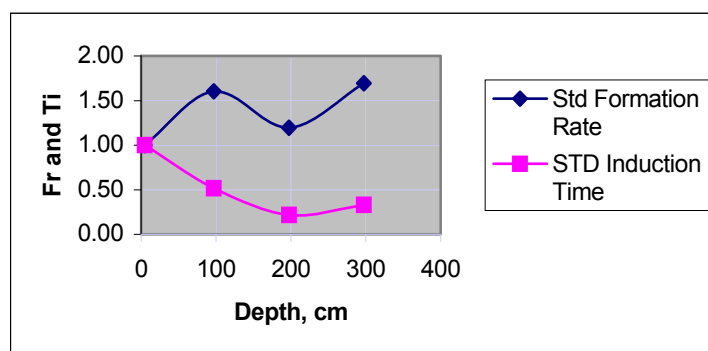


**Fig. 15.** Hydrate formation in Core 12, MC 118 ( $28^{\circ} 52.45$  N and  $89^{\circ} 29.2$  W)

## I. Laboratory Analysis of Cores from MC-118 Observatory Site

Samples from cores BC1, BC2, BC3, BC4, and BC9 were analyzed in the laboratory for hydrate formation rate and hydrate induction time. (A map of the Observatory Site is given in Fig. 16.) Sediments containing indigenous waters were mixed in the laboratory with Ottawa sand in the weight ratio of 75/25 sand/sediment to improve gas permeability, increase porosity of the packing, and increase mineral-gas contact. Pressures, temperatures, cooling rates, and gas compositions were kept constant during each analysis. These near-surface samples were taken from the MC-118 Observatory Site on June 9 and June 10, 2006, utilizing box cores.

Multiple experimental runs were made with each sample analyzed. Therefore, the average values of hydrate formation rate ( $Fr_{max}$ , mmol/h) and hydrate induction time ( $T_i$ , hours) in Table V for most cases are averages of 3 to 5 repetitive runs.

**TABLE V.** Composite results

Sample	$Fr_{max}$ , (mmol/h)	$T_i$ (hours)
BC-1	52.5	0.43
BC-2	53.4	0.49
BC-3	71.9	1.49
BC-4	64.0	1.35
BC-9	50.8	1.81

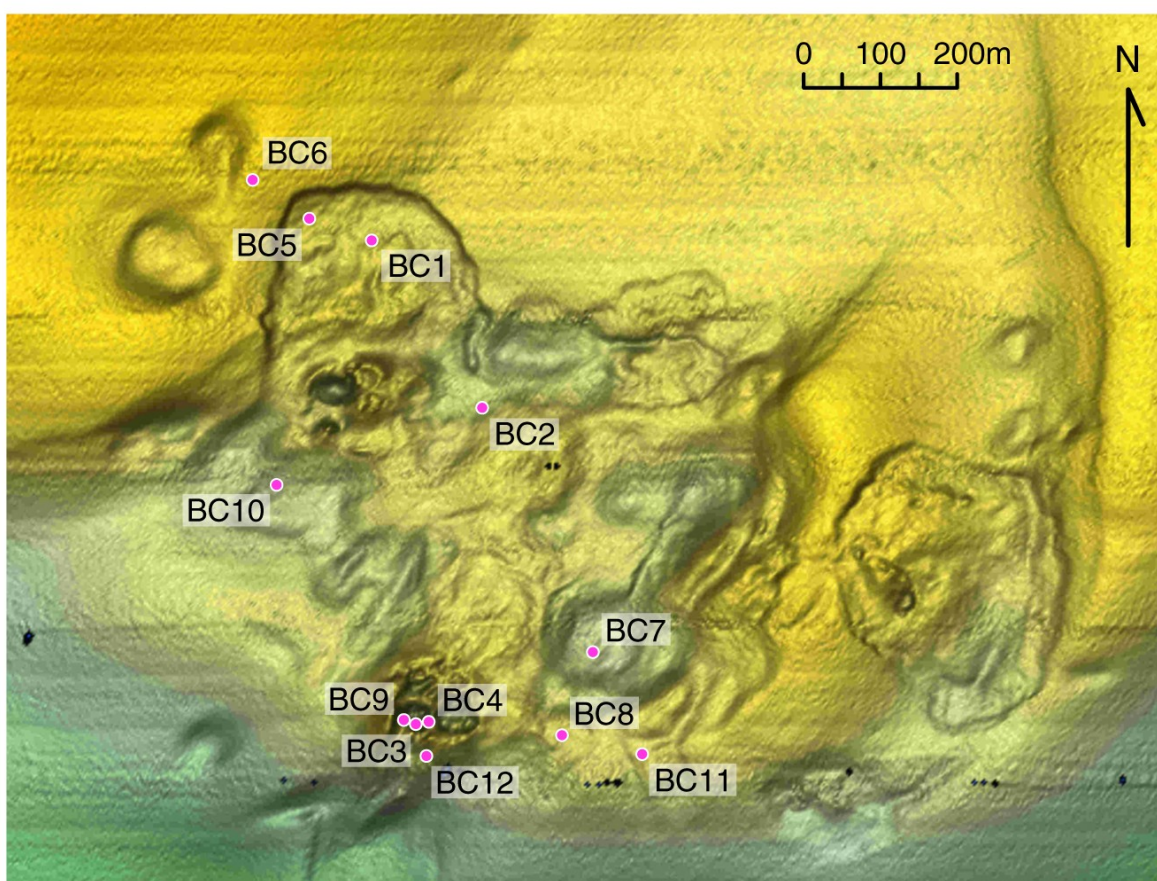


Fig. 16. Map of Observatory Site and location of samples analyzed.

As given in Fig. 17 and Fig. 18, formation rates and induction times are similar for the sets of cores BC1/BC2 and BC3/BC4. This observation is reasonable since the cores are in proximity to each other, as can be seen on the map of Fig. 16. In Fig. 18, Sample BC9 induction times are shown to be more distinctly unique. It may be noteworthy that only Sample BC9 is fairly saturated with crude oil. This covering of mineral surfaces with the oil could reduce nucleation sites.

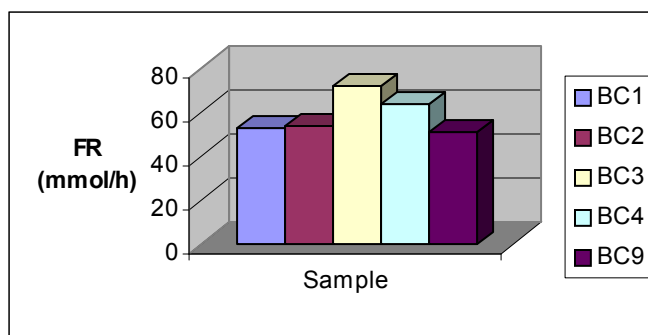


Fig. 17. Hydrate formation rates of sediments

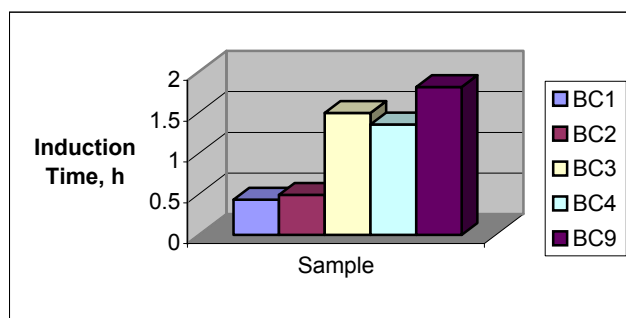


Fig. 18. Hydrate induction times of sediments.

## J. Publications of the Work

The following articles, based on the work of this grant, were published in refereed journals. Acknowledgements were made of DOE grant support through the Gulf Coast Gas Hydrate Consortium at the Mississippi Mineral Resources Institute of the University of Mississippi.

Dissertation research was done under the grant and one PhD was awarded as a consequence.

1. Rogers, R.E., Zhang, G., Dearman, J., Woods, C., "Investigations into surfactant/gas-hydrate relationship," *J. Petrol. Sci. & Tech.* **56** (2007) 82-88.
2. Zhang, G., Rogers, R.E., French, W. T., and Lao, W., "Investigation of microbial influence on seafloor gas-hydrate formations," *Marine Chemistry*. **103** (2007) 359- 369.
3. Kelleher, B.P., Simpson, A.J., Rogers, R.E., Dearman, J., and Kingery, W.L., "Effects of natural organic matter from sediments on the growth of marine gas hydrates," *Marine Chemistry*. **103** (2007) 237- 249.
4. Rogers, R.E., Sassen, R., Dearman, J.S., and Zhang, G., "Factors prompting seafloor experiments to investigate microbial/hydrate relationships," presented at 16<sup>th</sup> International Offshore and Polar Engineering Conference & Exhibition, San Francisco, May 28- June 2, 2006.

5. Dearman, J.L., Gas Hydrate Formation in Gulf of Mexico Sediments. Ph.D. dissertation, Mississippi State University, Swalm School of Chemical Engineering, April 9, 2007.

## V. CONCLUSIONS

### A. Dufresne MD02-2570 Cores of 30-m Depth

- a. A correlation exists between hydrate formation rate and depth of the sediments below seafloor. Hydrate formation rate in the sediments is most rapid at about 15- 18 m depth.
- b. A correlation exists between hydrate induction time and depth of the sediments below seafloor. Hydrate induction time reaches a minimum at about 12 m and remains at that very short induction time to the bottom of the core at 30 m.
- c. Silt, sand, and clay percentages in the sediments show trends with depth that suggest a contributing factor to the hydrate formation ease.
- d. Smectite, illite, chlorite, and kaolinite percentages in the sediments were determined. Smectite and illite may influence the hydrate formation trends found in the tests.

### B. Near-Surface Cores from Mississippi Canyon

Gas-hydrate formations vary as one moves laterally at near-surface depths of the seafloor in Mississippi Canyon. These near-surface variations usually differ from the distinct patterns of hydrate formation rates and induction times observed in the 30-m deep Dufresne core sediments. However, even the Dufresne sediments gave near-surface variations in hydrate formation. It is hypothesized that extent and depth of the sulfate zone is a primary cause of the variations, because in the sulfate zone a different microbial community exists along with different bioproducts. The depth of the sulfate zone varies with methane flux from below.

High salinity areas in the sediments were shown to retard hydrate formation.

Carbonate nodules in the sediments were significant. At these points, maximum formation rates and minimum induction times were observed.

### **C. Hydrate Nucleation Centers**

The work indicates that smectite clays promote hydrate formation by basic platelets sloughing off the clay mass and these small platelets act as nuclei for hydrate formation. Anionic bioproducts may collect in the interlayers of the platelets or on the platelet surfaces and also become involved in the mechanism of hydrate promotion.

It is thought that the variety of bioproducts existing with depth in the sediments may mask particle size effects—that is, some bioproducts may promote hydrates and others may coat particles and retard hydrate formation.

Sediments with crude oil exhibited longer hydrate induction times, probably because of covering nucleation sites.

### **D. Publications**

The DOE grants have allowed 4 articles to be published in national and international journals during the grant period.

The grant supported the dissertation research and awarding of the Ph.D. for one graduate student.

# **EXPERIMENT TO GENERATE SHEAR WAVES IN THE SEA FLOOR AND RECORD THEM WITH A HORIZONTAL LINE ARRAY**

## **PROGRESS REPORT**

**Paul Higley: Principal Investigator  
Specialty Devices, Inc.  
Wylie, Texas**

**May 30, 2007**



## **EXPERIMENT TO GENERATE SHEAR WAVES IN THE SEA FLOOR AND RECORD THEM WITH A HORIZONTAL LINE ARRAY**

The integration of the Input/Output (I/O) sensor to the Horizontal Line Array is desirable as the resolution, accuracy and low frequency response of this true digital sensor is superior to that of marine 3 axis geophone sensors. The root of the problem for use of this sensor has been the interface of the sensor to a non-I/O data collection system. I/O has developed this sensor as part of a highly integrated seismic system which can collect data from 10's of thousands of these sensors every 10 to 20 seconds. This requires very fast data transmission. I/O has developed a data interface that is both proprietary and elegant. Data collection is terminated at large truck-mounted computer systems with the capability to log the large data sets. The adaptation of portions of this data transmission scheme and repackaging and miniaturizing of this data-collection scheme is the major part of the effort necessary to integrate the sensors into the SFO data retrieval system. The advantages of this unique sensor package were deemed sufficient to warrant staying with the development of a way to integrate this sensor. Recent advances in the miniaturization of interface circuitry and support from I/O has resolved the remaining engineering tasks and trial collection of 4C data will be completed in June 2007.

During December of 2006 and January of 2007 the possibility of using a new I/O marine DigiSeis capability was investigated. The advantage of this system is the marine version of this sensor has a hydrophone integrated with the three axis accelerometer. Further discussions with I/O revealed that not only is the present hydrophone sample rate limited to 1 ms ( 1,000 sps) but the effort involved in redesigning the system to achieve the desired 10,000 sps rate is a project that would require more investment than the entire Downhole vertical array program is presently budgeted. As a result we must either accept sampling at a far slower rate on the hydrophone than previously desired or we should proceed with our plan of integrating the accelerometer sensor into the SDI DATS system and retaining the fast sampling hydrophone array developed for the water-column vertical array. The decision was made to stay with integration of the 3 component DigiSies sensor into the SDI DATS array. .

In an effort to simplify the data communications and control electronics I/O developed an SCI circuit card with a proprietary custom IC which combines the functions of a large amount of the custom circuitry in the recording truck. The efforts in the spring of 2007 have centered on utilizing this new approach to the problem. SDI is building additional circuitry and writing software to finally resolve this communications problem. The SCI card will communicate directly with SDI's present ALI cards with a software upgrade to the ALI cards. I/O completed the software upgrade in April. During May of 2007 SDI has been integrating the updated ALI circuitry and the new SCI card with communications software for system test and data collection. The power requirement of this system is now 12

vdc and 48 vdc. The 12 vdc will be generated from the PCB and with the modification of the PCB design in 2007 to 48 vdc from 24 vdc the 48 vdc can now be supplied to the data collection array without further conversion.

The new SCI circuitry has apparently cured the last of the problems for packaging this technology in a format that will lend itself to installation on the sea floor. The new combination of cards and software is being packaged and will be tested at sea with the MMRI Sled combination S and P wave source in June. This should represent the completion of the development of this Downhole array technology.

## ACRONYMS

<b>4-C</b>	four-component
<b>ALI</b>	A-Link interface (Input/Output's combination of units; accelerometer pseudo-ethernet communications interface and timing device)
<b>AUV</b>	autonomous underwater vehicle
<b>BC</b>	box core
<b>BCS</b>	Barrodale Computing Services, Ltd.
<b>C&amp;C</b>	Chance and Chance
<b>CH<sub>4</sub> (=CH<sub>4</sub>)</b>	methane
<b>cmbsf</b>	centimeters below sea-floor
<b>CMRET</b>	Center for Marine Resources and Environmental Technology
<b>CO<sub>2</sub> (=CO<sub>2</sub>)</b>	carbon dioxide
<b>DATS</b>	Data Acquisition and Telemetry System
<b>DI</b>	deionized
<b>DOC</b>	Department of Commerce
<b>DOE</b>	Department of Energy
<b>DOI</b>	Department of the Interior
<b>EGL</b>	Exploration Geophysics Laboratory
<b>FY</b>	Fiscal Year
<b>GOM</b>	Gulf of Mexico
<b>GOM-HRC</b>	Gulf of Mexico-Hydrates Research Consortium
<b>HLA</b>	horizontal line array
<b>HRC</b>	Hydrates Research Consortium
<b>HSZ</b>	Hydrate Stability Zone
<b>IC</b>	integrated circuit
<b>I-O; I/O</b>	Input-Output Corporation
<b>JIP</b>	Joint Industries Program
<b>mbsf</b>	meters below sea floor
<b>MC</b>	Mississippi Canyon
<b>MD</b>	Marion Dufresne
<b>mM</b>	millimolar
<b>MMRI</b>	Mississippi Mineral Resources Institute
<b>MMS</b>	Minerals Management Service
<b>MS/SFO</b>	monitoring station/sea-floor observatory
<b>M/V</b>	merchant vessel
<b>NETL</b>	National Energy Technology Laboratory
<b>NIUST</b>	National Institute for Undersea Science and Technology
<b>NOAA</b>	National Oceanographic and Atmospheric Administration
<b>NURP</b>	National Undersea Research Program
<b>OBC</b>	ocean-bottom cable
<b>OLW</b>	over-lying water
<b>PCB</b>	pressure-compensated battery
<b>PFA (=PCA)</b>	pore-fluid array
<b>P-P</b>	standard P-wave seismic data

<b>P-SV</b>	converted-shear mode (P-wave to SV-shear wave conversion)
<b>PVC</b>	polyvinyl chloride
<b>P-wave</b>	compressional wave
<b>ROV</b>	remotely operated vehicle
<b>RTD</b>	resistance temperature detector
<b>R/V</b>	Research Vessel
<b>SCI</b>	serial communications interface
<b>SDI</b>	Specialty Devices, Inc.
<b>SFO</b>	Sea Floor Observatory
<b>SFP</b>	Sea Floor Probe
<b>SSD</b>	Station Service Device
<b>SS/DR</b>	shallow-source/deep-receiver
<b>S-wave</b>	shear wave
<b>US</b>	United States
<b>USGS</b>	United States Geological Survey
<b>vdc</b>	volts direct current
<b>VLA</b>	vertical line array
<b>V<sub>p</sub></b>	P-wave velocity
<b>VSP</b>	vertical seismic profile